We are IntechOpen, the world's leading publisher of Open Access books Built by scientists, for scientists

6,900
Open access books available

186,000
International authors and editors

200M
Downloads

Our authors are among the

154
Countries delivered to

TOP 1%
most cited scientists

12.2%
Contributors from top 500 universities

CLARIVATE ANALYTICS

BOOK CITATION INDEX

INDEXED

WEB OF SCIENCE™

Selection of our books indexed in the Book Citation Index
in Web of Science™ Core Collection (BKCI)

Interested in publishing with us?
Contact book.department@intechopen.com

Numbers displayed above are based on latest data collected.
For more information visit www.intechopen.com

Magnetic Nanoparticles: Synthesis, Surface Modifications and Application in Drug Delivery

Seyda Bucak, Banu Yavuztürk and Ali Demir Sezer

Additional information is available at the end of the chapter

1. Introduction

Magnetic nanoparticles (MNP) have gained a lot of attention in biomedical and industrial applications due to their biocompatibility, easy of surface modification and magnetic properties. Magnetic nanoparticles can be utilized in versatile ways, very similar to those of nanoparticles in general. However, the magnetic properties of these particles add a new dimension where they can be manipulated upon application of an external magnetic field. This property opens up new applications where drugs that are attached to a magnetic particle to be targeted in the body using a magnetic field. Often, targeting is achieved by attaching a molecule that recognizes another molecule that is specific to the desired target area. This often requires a chemical recognition mechanism and does not succeed as designed. Therefore, magnetic nanoparticles can offer a solution to carry drugs to the desired areas in the body.

Magnetic nanoparticles, although may contain other elements, are often iron oxides. Most common iron oxides are magnetite (Fe_3O_4), maghemite (γ-Fe_2O_3), hematite (α-Fe_2O_3) and geotite. Depending on the experimental conditions, one or more of the iron oxide phases may form. It is very important to carefully control the experimental conditions to ensure the presence of a single-phase.

Frequently encountered iron oxide nanoparticles in applications are superparamagnetic. Superparamagnetism is a form of magnetism, which is observed with small ferromagnetic or ferrimagnetic nanoparticles. In small enough nanoparticles, magnetization can randomly flip direction of nanoparticle under the influence of temperature. However, the magnetic susceptibility of superparamagnetic nanoparticles is much larger than the paramagnetic ones. Superparamagnetism occurs in nanoparticles that have single-domain, i.e. composed of a single magnetic domain. In this condition, it is considered that the magnetization of the nanoparticles is a single-giant magnetic moment, the sum of all the individual magnetic

moments carried by the atoms of the nanoparticle. When an external magnetic field is applied to the superparamagnetic nanoparticles, they tend to align along the magnetic field, leading to a net magnetization. In the absence of an external magnetic field, however, the dipoles are randomly oriented and there is no net magnetization. The size dependence of magnetic properties of Fe_3O_4 nanoparticles synthesized from non-aqueous homogeneous solutions of polyols has been recently investigated (Caruntu et al., 2007). Out of the previously mentioned iron oxides, magnetite and maghemite are superparamagnetic and studies where these are used as magnetic nanoparticles will predominantly be focused in this summary.

Recent toxicity studies on magnetic nanoparticles are summarized to show the biocompatibility of these particles. Research on targeting drugs using MNPs show to be very promising and some examples are given. Hyperthermia, which is a complementary treatment for tumors that uses magnetic field to increase temperature and cause cell death, can be achieved using MNPs and some recent advances in this field are presented. At the end, a table summaries different types of MNP matrixes used for drug delivery applications.

2. Toxicity

One of the main reasons that made magnetic nanoparticles interesting for biomedical applications is their biocompatibility. As these particles are being used as drug delivery vehicles, their cytotoxicity should be investigated in detail. These particles have been shown to have low toxicity in human body by several *in vitro* and *in vivo* studies.

Ferric iron is normally transported by means of transferrin, which can bind the cell-surface localized transferrin receptor. Within the cell cytoplasm, the majority of the cytoplasmic iron pool is stored in specialized proteins called ferritin. Due to the physiological relevance of iron, MNPs were initially considered to be non-cytotoxic. MNPs can naturally be broken down resulting in the release of ferric iron which can then participate in the normal iron metabolism. It has, however, been recognized that the small size of MNPs might pose an additional hazard as the particles can reach high local concentrations within the cells and are generally more difficult to be efficiently cleared from the body (Rivera et al., 2010; Chan et al., 2002). Furthermore, free iron has been associated with the formation of free radicals, which would be particularly harmful to neural tissues already weakened by pathological processes (Winer et al., 2011).

It is important to note that in almost all the studies, the toxicity is shown to increase significantly above a certain administration level. Although high loadings (>100 μg/mL) of MNPs cause cytotoxicity, the concentrations needed for drug delivery applications are often below the toxic level for suitably coated MNPs (Karlsson et al., 2008).

Toxicity is often a result of serum proteins binding to the surface of the MNPs, altering the composition of the cell medium to which the cells are exposed (Mahmoudi et al., 2009). Coated nanoparticles induce lower toxicity not only due to the presence of the biocompatible coating, but also due to the lower adsorption sites for proteins, ions and other components in the medium (Mahmoudi et al., 2010).
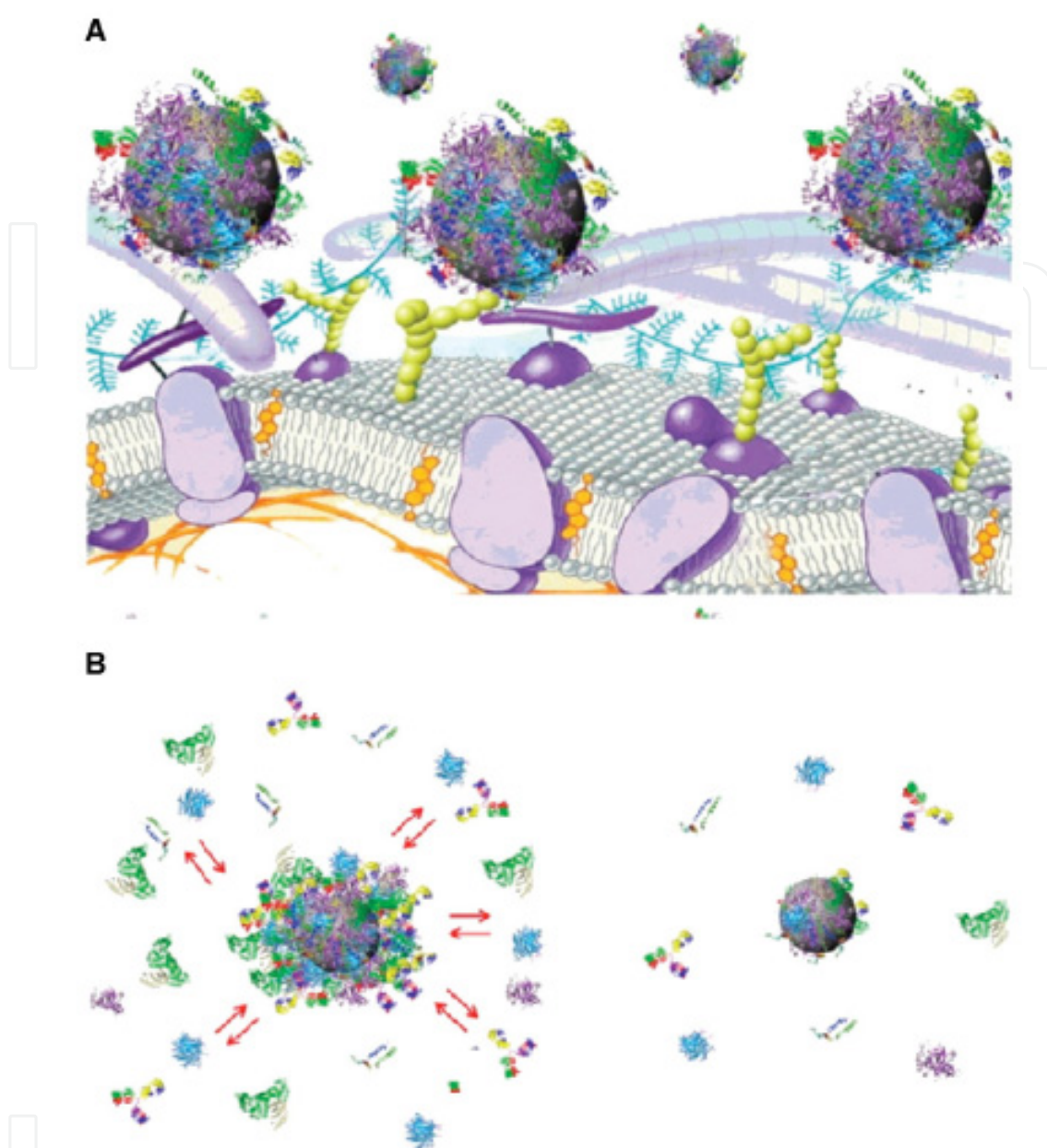
Figure 1. (A) Schematic representation of the possible exchange/interaction scenarios at the bionanointerface at the cellular level. (B) Schematic drawing of the structure of protein–nanoparticle in blood plasma confirming the existence of various protein binding (e.g. an outerweakly interacting layer of protein (full red arrows) and a hard slowly exchanging corona of proteins (right) (Mahmoudi et al., 2011)

Magnetite (Fe_3O_4) and maghemite (γ-Fe_2O_3) can show different cellular responses because of their ability to undergo oxidation/reduction reactions. In fact, magnetite has been shown to cause higher levels of oxidative DNA lesions (using comet assay) in A549 human lung epithelial cell line in the absence of decreased cell viability as compared to maghemite owing to its potential to undergo oxidation (Karlsson et al., 2009; Karlsson et al., 2008).

One of the most sensitive parameters in toxicity is the surface coating of the nanoparticles. The degree of surface coverage has been postulated to be the main parameter in cellular

uptake as incomplete surface coverage was shown to promote opsonization and rapid endocytosis whereas fully coated MNPs escaped opsonization which, as a result, prolonged plasma half-life (Jung et al., 1995). The negatively charged uncoated MNPs have been shown to exhibit cytotoxicity above a certain threshold amount. Uncoated MNPs also have low solubilities which result in their precipitation in aqueous media impeding blood vessels in *in vivo* studies. In order to reduce the toxicity of MNPs, different coatings have been used. Häfeli at al. (Häfeli et al., 2009) have coated MNPs with polyethylene oxide (PEO) triblock copolymers (PEO-COOH-PEO) and found that the PEO tail block length inversely correlates with toxicity. PEO tail lengths above 2 kDa were suggested to be suitable for *in vivo* applications. Mahmoudi et al. (Mahmoudi et al., 2009) showed that uncoated particles induce greater toxicity than polyvinyl alcohol (PVA) coated magnetite particles. They also have shown that the toxicity of uncoated particles may significantly be reduced by substitution with surface-saturated uncoated particles. Coating maghemite particles with dimercaptosuccinic acid (DMSA) were shown to almost eliminate the toxicity of these particles (Auffan et al., 2006) by preventing direct contact between the particle and human dermal fibroblasts. However, in a different study using DMSA coated maghemite particles, a quantifiable model cell system is developed and showed that intercellular delivery of even moderate levels of MNPs may adversely affect cell function (Pisanic et al., 2007). Maghemite particles were coated with polyethylene imine (PEI)-g-polyethylene glycol (PEG) and their toxicity was compared with branched PEI coatings (Schweiger et al., 2011). Introduction of PEG was shown to have a shielding effect and resulted in lower toxicity Lee et al. (Lee et al., 2011) used ethylene glycol double layer stabilized maghemite nanoparticles and showed these to be non-toxic. PEG coating of magnetite particles also were shown to reduce the toxicity (Zhou et al., 2011).

When MNPs are embedded in chitosan to obtain magnetic chitosan particles, they have shown to exhibit relatively low cytotoxicity (Park et al., 2005) due to complete coverage of MNPs with chitosan.

Although dextran is a complex branched glucose that is often used in medical applications, dextran coated magnetite particles caused cell death as much as uncoated magnetite particles (Berry et al., 2003). Conversely, in a comparative study, uncoated magnetite, uncoated maghemite, dextran coated magnetite and dextran coated maghemite were investigated for cytotoxicity and neither of the samples exhibited cytotoxicity below 100 mg/mL and the only samples that demonstrated genotoxicity was the dextran coated maghemite (Singh et al., 2012). In a more extensive study, Ding et al. (Ding et al., 2010) showed that the cytotoxicity of dextran hybridized magnetite nanoparticles is cell-specific. This result suggests that the related cells should be concerned for the cytotoxicity evaluation.

A range of secondary surfactants around magnetic particles have been tested for toxicity *in vivo*. Citric and alginic acid surfactants were found to be significantly less toxic than starch, decanoic acid and PEG. This study shows the importance of optimizing surface coating to minimize toxicity (Kuznetsov et al., 1999).

In an *in vivo* study, albumin coated magnetite microspheres were shown to be well tolerated (Kuznetsov et al., 1999) Magnetite albumin microspheres bearing adriamycin (an anti-cancer drug) showed reduced toxicity to animal organs or cells compared to a single dose of adriamycin which reduces the side effects remarkably (Ma et al.,2000). However, in another study, albumin derivatized MNPs were found to cause membrane disruption, possibly due to the interaction of the protein with membrane fatty acids and phospholipids (Berry et al., 2003).

Low cytotoxicity compared to uncoated magnetite particles was evaluated of Fe_3O_4–PLLA–PEG–PLLA (PLLA: poly L-lactic acid) particles at the cellular level. They also create low genotoxic and immuntoxic at the molecular level. Acute toxicity tests showed quite a low toxicity which makes them have great potential for use in biomedical applications (Chen et al., 2012). Magnetite encapsulated in micelles of MPEG-PLGA (PLGA: poly (lactic-co-glycolic acid) exhibited no cytoxicity (Ding et al., 2012).

More recently, particle size as opposed to coating degree has been suggested to exert chief influence on the rates of uptake by macrophages (Raynal et al., 2004). In *in vivo* studies, MNPs of 50 nm (dextran coated) and 4 µm (polystyrene coated) were used and shown to be safe for intraocular applications (Raju et al., 2011). Oral, intravenous and intraperitoneal administration of MNPs of about 20 nm did not exhibit toxicity (Zefeng et al., 2005). MNPs with 1,6 hexanediamine were shown to be safe after being administered by intracerebral or intraarteral inoculation to rats (Muldoon et al., 2005). MNPs of 40 nm were shown to be non-toxic to mES cells (Shundo et al., 2012).

Under the application of magnetic field, MNPs were shown to exhibit higher toxicities which lead to cell death (Simioni et al., 2007; Bae et al., 2011). This is the basis of a tumor treatment, hyperthermia, which will be summarized in detail in the later sections.

Despite such routine use of MNPs, the long-term effects and potential neurotoxicity have, as yet, not been evaluated extensively (Yildirimer et al., 2011).

The ability to use magnetic nanoparticles in biomedical applications due to their low cytotoxicity, stirred a big interest in the scientific community to use these particles as drug carriers. In drug delivery, there are mainly two goals; first is the targeting of the drug to the desired area in the body to reduce the side effects to other organs and second is the controlled release of the drug to avoid the classical overdosing/underdosing cycle. Magnetic nanoparticles may provide a solution to both these goals. The coating around the magnetic nanoparticle is optimized to carry and release the drug in the desired fashion, like in the case of most nanoparticles. However, the unique property of these particles is that they are magnetic, allowing being manipulated using an external magnetic field. This forms the basis of magnetic targeting where the drug-carrying magnetic particle is directed to a specific area upon application of a magnetic field.

3. Magnetic targeting

In order to investigate the magnetic targeting *in vitro*, an experimental setup that models a branched artery supplying a tumor region with parameters close to the real system has been

constructed. The targeting of the particles was achieved and found to be dependent on the magnetic volume force in the branch point (Gitter et al., 2011). Using the same set-up, a novel quantitative targeting map that combines magnetic volume forces at characteristic points, the magnet position and quantitative data was constructed. Up to 97% of the nanoparticles were successfully targeted into the chosen branch (Gitter et al., 2011).

A device for magnetically targeted drug delivery system (MT-DDS), which can allow to navigate and to accumulate the drug at the local diseased part inside the body by controlling to magnetic field strength and/or gradient generated by the superconducting magnets was developed. Mn-Zn ferrite particles are injected to an experimental apparatus as a vein model of the Y-shaped glass tubes using multiple bulk superconductor magnets. This is a basic technology for magnetically targeted drug delivery system that provides the drug navigation in the blood vessel of the circulatory organs system, which shows the usefulness of the medicine transportation methodology for MT-DDS (Mishima et al., 2007).

To test seeding MNP in blood vessels and targeting the injected ones to these specific sites, experimental and computational models are constructed. To create strong and localized field gradients, microfluidic channels embedded with magnetic anchors were constructed using modified soft lithographic techniques to analyze the trapping process. Qualitative results from experimental investigations confirmed the legitimacy of the approach. It is demonstrated that capturing and aggregating magnetic microspheres at specified points in the vascular system is possible (Forbes et al., 2003).

Locally targeted drug delivery using two magnetic sources was theoretically modeled and experimentally demonstrated as a new method for optimizing the delivery of magnetic carriers in high concentration to specific sites in the human body. Experimental results have demonstrated that capturing superparamagnetic beads of both micrometer and sub-micrometer diameter at reasonably high concentrations is possible in flow conditions consistent with the dimensions and flow velocity occurring in the coronary artery in the human body. The same experiments performed with non-magnetic mesh resulted in no significant capture, indicating that the implant is responsible for providing the necessary magnetic field gradients and forces to capture the injected beads (Yellen et al., 2005).

There are several *in vivo* studies on magnetic targeting. Magnetic chitosan nanoparticles, were successfully targeted to tumor tissue for photodynamic therapy, resulting in low accumulation in skin and hepatic tissue (Sun et al., 2009).

Magnetic carbon nanotubes (MNT) with a layer of magnetite nanoparticles on their inner surface were prepared where the chemotherapeutic agents were incorporated into the pores. By using an externally placed magnet to guide the drug matrix to the regional lymph nodes, the MNTs are shown to be retained in the draining targeted lymph node for several days and continuously release chemotherapeutic drugs (Yang et al., 2008).

In an *in vitro* study, magnetic poly(ethyl-2-cyanoacrylate) (PECA) nanoparticles containing anti-cancer drugs were shown to release drug and have magnetic mobility under external magnetic field (Yang et al., 2006).

Intra-caroid administration of polyethyleneimine (PEI) modified magnetic nanoparticles in conjunction with magnetic targeting resulted in 30 fold increase in tumor entrapment of particles compared to that seen with intravenous administration (Chertok et al., 2010).

Magnetite-dextan composite particles were employed to deliver mitoxantrone *in vivo*. Mitoxantrone concentration in tumor tissue was found to be always significantly higher with magnetic targeting and the plasma iron concentrations fell after the application of the magnet, indicating the effectiveness of magnetic targeting (Krukemeyer et al., 2012).

In another study, mitoxantrone was bound to superparamagnetic Fe_3O_4-nanoparticles and the drug loaded nanoparticles were given through the femoral artery close to the tumor. The magnetic nanoparticles were attracted to the tumors by a focused external magnetic field during the application. Results from HPLC-biodistribution experiments showed that magnetic drug targeting allows to enrich the therapeutic agent up to 50 times higher in the desired body compartment (i.e. the tumor region) compared to the commonly used systemic application (Alexiou et al., 2011).

Magnetic nanoparticle seeds composed of magnetite carboxyl modified polydivinylbenzene and containing magnetite were studied *in vitro* for use as an implant in implant assisted-magnetic drug targeting (IA-MDT). In the presence of a 70mT external magnetic field, the MNP seeds were captured first from a fluid stream passing through a 70% porous polymer scaff old that was designed to mimic capillary tissue. This is then used to capture magnetic drug carrier particles (MDCPs) with the same magnetic field (Mangual et al., 2011).

Poly-[aniline-co-N-(1-one-butyric acid) aniline] (SPAnH) coated Fe_3O_4 particles with 1,3-bis(2-chloroethyl)-1-nitrosourea (BCNU). Bound-BCNU-3 could be concentrated at targeted sites *in vitro* and *in vivo* using an externally applied magnet. When applied to brain tumors, magnetic targeting was found to increase the concentration and retention of bound-BCNU-3 (Hua et al., 2011).

The accumulation of superparamagnetic nanoparticles with starch coating in gliosarcomas were enhanced by magnetic targeting and quantified by MR imaging (Chertok et al., 2008).

PEG-modified cross linked starch coated magnetite particles for magnetic targeting studies *in vivo*. Selective, enhanced brain tumor targeting of intravenously administered PEG-MNPs was confirmed in a 9L-glioma rat model. Tumor targeting results, were promising and warranted both the further development of drug-loaded PEG-MNPs and concurrent optimization of the magnetic targeting strategy utilized (Cole et al., 2011).

Super high-magnetization nanocarriers (SHMNCs) comprising of a magnetic Fe_3O_4 (SHMNPs) core and a shell of aqueous stable self-doped poly[N-(1-onebutyric acid))aniline (SPAnH), which have a high drug loading capacity (27.1 wt%) of doxorubicin (DOX) were prepared. These nanocarriers enhanced the drug's thermal stability and maximized the efficiency with which it is delivered by magnetic targeting therapy to MGH-U1 bladder cancer cells, in part by avoiding the effects of p-glycoprotein (P-gp) pumps to enhance the intracellular concentration of DOX (Hua et al., 2011).

Magnetic particles are also targeted to tumor area so tumors can be imaged. Iron oxides particles are often used as contrast agents for MRI. In fact, magnetite is an FDA approved contrast agent. In this summary, magnetic particles used for MRI will not be covered as the focus of this study is to make a comprehensive summary on magnetic drug delivery.

As seen in the abovementioned studies, magnetic targeting is an efficient way to target drugs to the desired area, commonly to tumors. However, in some studies along with magnetic targeting, targeting ligands are also used. In the absence of magnetic targeting, targeting is achieved using ligands on drug carriers that specifically bind to receptors in the targeted area. A common ligand used for this purpose is folate (or folic acid). Folate has a high affinity for the folate receptor protein which is commonly expressed on the surface of many human cancers. If folate is tagged to a drug carrying nanoparticle, the folate binds to the folate receptor on the surface of cancer cell and the conjugate is uptaken via endocytosis, completing the targeted drug delivery. A schematic representation of a magnetic particle with targeting ligands is shown in Figure 2.
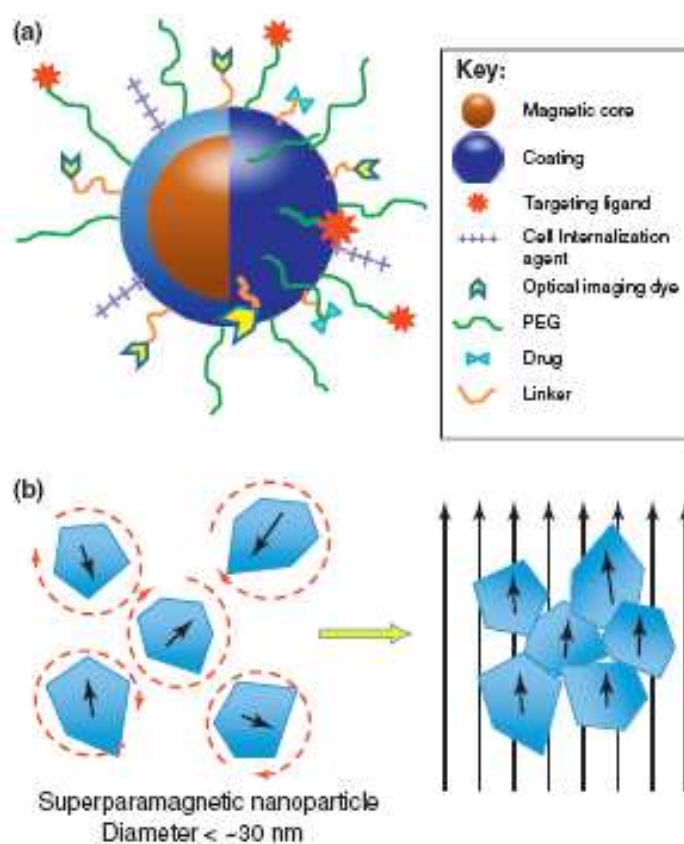
Figure 2. (a) Schematic representation of the ''core–shell'' structure of MNPs and multi-functional surface decoration. MNPs consist of a magnetic iron oxide core coated with a biocompatible material (e.g. polysaccharide, lipid, protein, small silane linkers, etc.). Functional groups on the surface of coatings are often used to link ligands for molecular targeting, cellular internalization, optical imaging, enhanced plasma residence and/or therapy. The variety of moieties that decorate the MNP surface imparts the nanoparticle with its multi-functional, theranostic character. (b) Illustration of superparamagnetic MNP response to applied magnetic fields. MNPs comprise rotating crystals that align with the direction of an applied magnetic field. Crystal reorientation provides the high magnetic

susceptibility and saturation magnetization observed for this material. The circular dashed lines around the superparamagnetic nanoparticles on the left illustrate the randomization of their orientation, due to temperature effects, in the absence of a magnetic field. (Cole et al.2011).

Magnetic nanocarriers were synthesized based on superparamagnetic iron oxide particles with biocompatible Pluronic F127 and poly(dl-lactic acid) (F127-PLA) copolymer chemically conjugated with folic acid (FA), carrying DOX. Magnetic particles were guided to targeted site by the aid of external magnetic field, and correspondingly the therapeutic efficacy of anti-tumor drug can be improved. These qualitative results were carried out with simply statistical analysis, which suggested that the dual targeting mechanisms can lead to better therapeutic results (Huang et al., 2012).

Superparamagnetic iron oxide nanocrystals and DOX are co-encapsulated into PLGA/polymeric liposome core–shell nanocarriers withcholesterol with or without folate. The folate-targeting DOX loaded magnetic core–shell nanocarriers were shown to have better targeting effect to the Hela cells *in vitro* than their non-folate targeting counterparts (Wang et al., 2012).

Thermosensitive magnetic liposomes with DPPC:cholesterol:DSPE-PEG2000:DSPE-PEG2000-Folate (DPPC: Dipalmitoylphosphatidylcholine; DSPE: 1,2-distearoyl-sn-glycero-3-phosphoethanolamine) at 80:20:4.5:0.5 molar ratio were prepared containing DOX. This carrier, when physically targeted to tumor cells in culture by a permanent magnetic field yielded a substantial increase in cellular uptake of DOX as compared to Caelyx® (a commercially available liposomal doxorubicin preparation), non-magnetic folate-targeted liposomes (FolDox) and free DOX in folate receptor expressing tumor cell lines (KB and HeLa cells) (Pradhan et al., 2010).

Magnetic nanoparticles with mesoporous core-shell structure of silica were prepared and successfully modified with a fluorescent polymer chain as a labeling segment and folic acid as the cancer targeting moiety and loaded with a drug for directional release. The drug carrier was shown to be able to drill into the cell membranes and obtain a sustained release of the anticancer drug into the cytoplasm. The *in vitro* cellular uptake of the drug demonstrated that the drug-loaded nanocomposites could effectively target the tumor cells (Chen et al., 2010).

Nanoparticles of Fe_3O_4 core with fluorescent SiO_2 shell were synthesized and grafted with hyperbranched polyglycerol (HPG-grafted $Fe_3O_4@SiO_2$ nanoparticles) conjugated with folic acid. Significant preferential uptake of the folic acid-conjugated nanoparticles by human ovarian carcinoma cells (SKOV-3) as compared to macrophages and fibroblasts were shown by *in vitro* studies (Wang et al., 2011).

Magnetite nanoparticles are decorated through the adsorption of a polymeric layer (carboxymethly chitosan) around the particle surface and are conjugated with fluorescent dye, targeting ligand, and drug molecules for improvement of target specific diagnostic and possible therapeutics applications. Acrylic acid, folic acid, particles (Fe_3O_4-CMC-AA-FA) and DOX was loaded into the shell of the MNPs and release study was carried out at

different pH. The Fe₃O₄-CMC-AA-FA-DOX NPs showed a significant growth inhibition for HeLa cells in a dose dependent manner in comparison to NIH3T3 cells. This study indicates that Fe₃O₄-CMC-AA-FA is able to provide a single nanoscale construct, which is capable of tumor cell-targeting, imaging, and drug delivery functions. This is the first description of a chitosan based MNPs system possessing all of the above mentioned capabilities (Sahu et al., 2012).

Other ligands than folate have also been used for active targeting of nanoparticles. DOX on 5-carboxylfluorescein (FAM) labeled AGKGTPSLETTP peptide (A54) coupled starch-coated iron oxide nanoparticles demonstrated the specificity of DOX-loaded A54-SIONs (SION: superparamagnetic iron oxide) to BEL-7402 cells *in vitro*. The microscopy images proved that DOX-loaded A54-SIONs were successfully targeted to tumor tissue of nude mice with an external magnetic field *in vivo* (Yang et al., 2009).

Ligand-modified CPT-SAIO@SiO₂ nanocarriers were used for the delivery of an anticancer agent (encapsulated camptothecin (CPT)). It was found that the modified nanocarriers showed reasonably high drug load efficiency for CPT and a high uptake rate by cancer cells overexpressing EGFR through clathrin-mediated endocytosis. The intracellular release of the CPT molecules via an external magnetic stimulus proved to be technically successful and ensured much higher therapeutic efficacy than that obtained with the free drug (Tung et al., 2011).

Cetuximab-immuno micelles in which the anti-EGFR (Epidermal growth factor receptor) (EGFR), monoclonal antibody was linked to poly(ethylene glycol)-block-poly(ε-caprolactone) (PEG–PCL) These micelles were loaded with DOX and Fe₃O₄ superparamagnetic iron oxide. It was demonstrated that the immunomicelles inhibited cell proliferation more effectively than their nontargeting counterparts. Cetuximab-immunomicelles bind more efficiently to the cancer cells that overexpress epidermal growth factor receptor, leading to a higher quantity of superparamagnetic iron oxide and DOX being transported into these cells (Liao et al., 2011).

An anticancer drug was conjugated onto the PEGylated SPIO (SPIO: superparamagnetic iron oxide) nanocarriers via pH-sensitive bonds. Tumor-targeting ligands, cyclo(Arg-Gly-Asp-D-Phe-Cys) (c(RGDfC)) peptides, and PET 64Cu chelators, macrocyclic 1,4,7-triazacyclononane-N, N0, N00-triacetic acid (NOTA), were conjugated onto the distal ends of the PEG arms. cRGD-conjugated SPIO nanocarriers exhibited a higher level of cellular uptake than cRGD-free ones *in vitro*. These nanocarriers demonstrated promising properties for combined targeted anticancer drug delivery and PET/MRI dual-modality imaging of tumors (Yang et al., 2011).

Polymeric liposomes (PEG/RGD-MPLs); composed of amphiphilic polymer octadecyl-quaternized modified poly (γ-glutamic acid) (OQPGA), PEGylated OQPGA, RGD peptide grafted OQPGA and magnetic nanoparticles. It provided a possibility to responded to external permanent magnet with superparamagnetic characteristics, when was used for magnetic tissue targeting *in vivo*. The cell uptake results suggested that the PEG/RGDMPLs

(with RGD and magnetic particles) exhibited more drug cellular uptake than non RGD and non magnetism carriers in MCF-7 cells (Su et al., 2012).

All these studies show that magnetic targeting is an efficient way to target drugs to tumor area. Coupled with active targeting using appropriate ligands, ligand-modified drug loaded magnetic nanoparticles, upon application of an external magnetic field provide excellent systems for effective drug targeting. Once targeting of magnetic particles to the desired area takes place, one of the most frequently used tumor treatments is hyperthermia. When magnetic nanoparticles are in the vicinity of the tumor and are subjected to an alternating magnetic field, dissipate heat and raise the temperature of the tumor, resulting in tumor cell death.

4. Hyperthermia treatment

Temperatures between 40°C and 45°C are generally being referred to as hyperthermia. Temperatures up to 42°C can render cancer cells more susceptible to the effect of irradiation and cause a certain degree of apoptosis, whereas temperatures >45°C are termed thermoablation and cause direct cell killing (necrosis) (Elsherbini et al., 2011).

In clinical applications of magnetic nanoparticle hyperthermia for cancer treatment it is very important to ensure a maximum damage to the tumor while protecting the normal tissue (Salloum et al., 2009). Although magnetic nanoparticle hyperthermia in cancer treatment holds great potential, it is severely limited by the fact that the anticipated heating distribution is difficult to control, and it leads to uneven and inadequate temperature elevation in tumor tissue. Transport of particles in tissue involves processes including extracellular transport of the carrier solution, transport of particles in the carrier solutions, and interaction between the particles and cell surface. The extracellular transport of nanoparticles in tumors is not well understood (Salloum et al., 2008).

Hyperthermia is almost always used with other forms of cancer therapy, such as radiation therapy and chemotherapy. Hyperthermia may make some cancer cells more sensitive to radiation or harm other cancer cells that radiation cannot damage. When hyperthermia and radiation therapy are combined, they are often given within an hour of each other. Hyperthermia can also enhance the effects of certain anticancer drugs (Van der Zee, 2002; Wust et al., 2002).

Numerous clinical trials have studied hyperthermia in combination with radiation therapy and/or chemotherapy. These studies have focused on the treatment of many types of cancer, including sarcoma, melanoma, and cancers of the head and neck, brain, lung, esophagus, breast, bladder, rectum, liver, appendix, cervix, and peritoneal lining (mesothelioma) (Falk et al., 2001; Feldman et al., 2003; Chang et al., 2001). Many of these studies, but not all, have shown a significant reduction in tumor size when hyperthermia is combined with other treatments. However, not all of these studies have shown increased survival in patients receiving the combined treatments (Van der Zee, 2002; Wust et al., 2002).Unique advantages of magnetic nanomaterials for hyperthermia based and combined therapies are schematically shown in Figure 3.
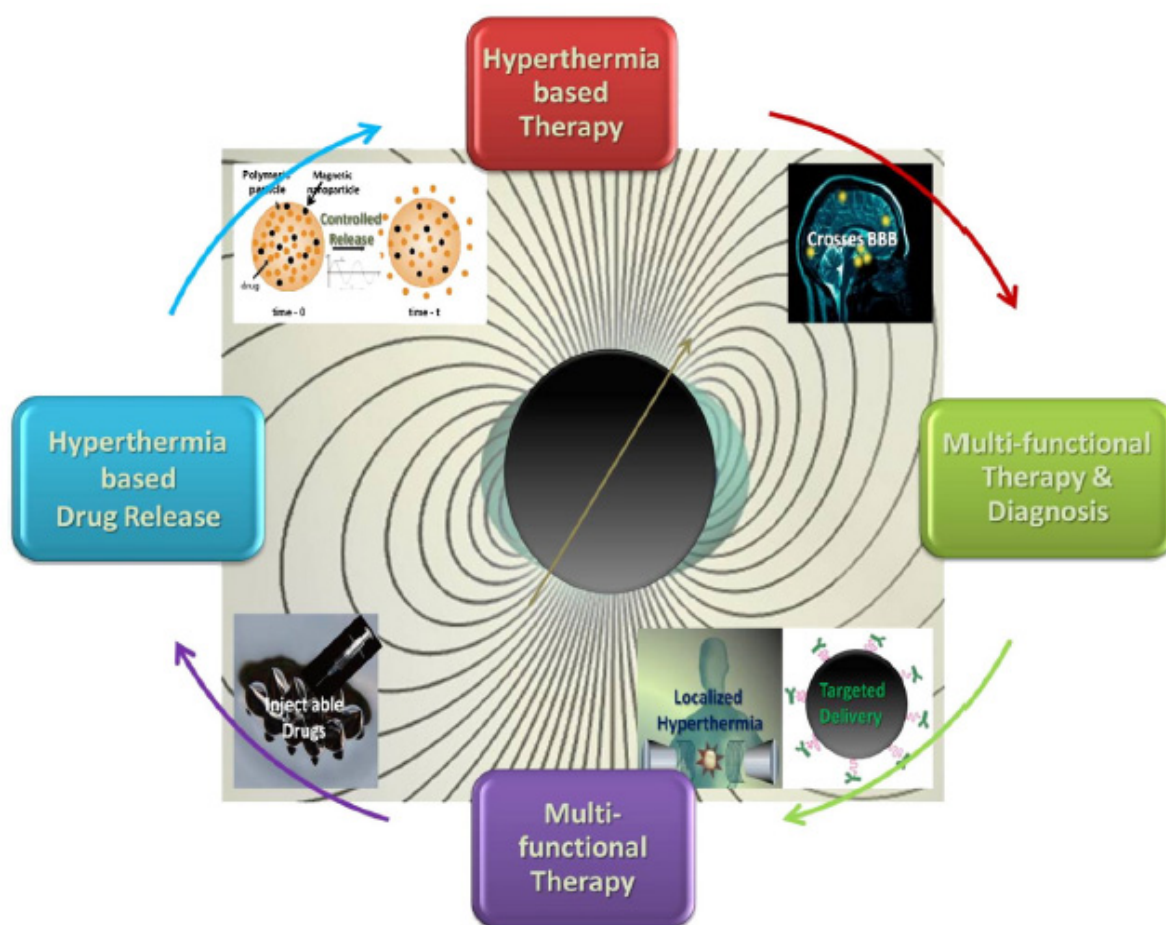
Figure 3. A schematic representation of some of the unique advantages of magnetic nanomaterials for hyperthermia-based therapy and controlled drug delivery (Kumar & Mohammad, 2011).

Magnetic losses in an alternating magnetic field to be utilized for heating arise due to different processes of magnetization reversal in the particle system: (1) hysteresis, (2) Néel or Brown relaxation, and (3) frictional losses in viscous suspensions (Hergt et al., 2006).

The magnetization of superparamagnetic nanoparticles can spontaneously change orientation under the influence of thermal energy. The magnetization oscillates between its two equilibrium positions. The typical time between two orientation changes is given by the Néel relaxation time $\tau_N = \tau_0 e^{\frac{KV}{k_B T}}$, where τ_0 is an attempt time with a value around 10^{-9}-10^{-10} seconds.

In the absence of a magnetic field, magnetic nanoparticles in solution move randomly, a movement called Brownian motion. When magnetic field is applied to magnetic nanoparticles in a fluid, magnetic nanoparticles rotate and progressively align with the magnetic field due to the torque generated by the interaction of the magnetic field with the magnetization. The time taken for a magnetic nanoparticle to align with a small external magnetic field is given by the Brown relaxation time: $\tau_B = \frac{3\eta V}{k_B T}$, where η is the solvent viscosity. The delay between the magnetic field rotation and the magnetization rotation

leads to a hysteresis. The area of this hysteresis loop is dissipated in the environment as thermal energy, which used in magnetic hyperthermia.

When an alternating magnetic field (AMF) is applied to a magnetic material, due to magnetic hysteresis, an energy is dissipated called the Specific Absorption Rate (SAR) and is expressed in W/g of nanoparticles.

The *SAR* of a given material is given by *SAR = Af*, where *A* is the area of the hysteresis loop and *f* the alternation frequency of the magnetic field. *A* is expressed in J/g and is also called the "specific losses" of the material, hence SAR may also be referred to as Specific Loss Power (SLP) in some studies.

The value of SAR estimated for the same material by several research groups may vary because it depends on several parameters like the physical and chemical properties of the carrier fluid, coating materials, frequency and amplitude of applied field, size and shape of Fe_3O_4 nanoparticles (Elsherbini et al., 2011).

An optimized SAR distribution in terms of A is developed by optimizing an algorithm to inversely determine the optimum heating patterns induced by multiple nanoparticle injections (Salloum et al., 2009). For hyperthermia applications, high SAR values are required. One way to achieve this is to increase the magnetic field strength but the average magnetic field strength should be kept below 30 mT to avoid the formation of eddy currents, which can induce toxicity (Alphandéry et al., 2012).

The study of SPA as a function of particle size shows that the average size and size distribution of the nanoparticles constituting a heating agent are central parameters for the design of efficient heating nanoparticles (Goya et al., 2008).

Unfortunately a direct comparison of particle composition and size is very difficult to make. In one study multidomain ferrite particles were prepared and SAR data is compared with small magnetite particles with and without dextran coating. Large ferrite particles (200-400 nm) had considerably lower power absorption per mass than smaller particles of the same composition although both particle size distributions were relatively broad (Jordan et al., 1993). However particles with large sizes are shown not reach inner cell (Martín-Saavedra et al., 2010).

By performing calorimetry measurements with Pluronic F127 coated Fe_3O_4 monodisperse particles it was shown that at a given frequency, heating rates of superparamagnetic particles are dependent on particle size, in agreement with earlier theoretical predictions. Results also indicate a broadening of SLP with sample polydispersity as predicted (Gonzales-Weimuller et al., 2009).

Similarly, a mean particle diameter in the single domain size range (20–70 nm) combined with a small size distribution width are shown to enhance SLP (Hergt et al., 2007).

Previous studies have shown a linear relationship between tissue iron concentration and heating rate in targeted magnetic hyperthermia treatment (Pardoe et al., 2003). A critical component of arterial embolization hyperthermia (AEH) is shown to be the concentration and distribution of ferromagnetic particles in the normal hepatic parenchyma (NHP), as well as in

the tumor tissue. If the distribution of particles in NHP is heterogeneous, with areas of high concentration, then unwanted areas of necrosis may result during AEH (Moroz et al., 2002).

In another study, several types of magnetic iron oxide nanoparticles representative for different preparation methods (wet chemical precipitation, grinding, bacterial synthesis, magnetic size fractionation) are used for a comparative study (Hergt et al., 2006). Commercially available very small superparamagnetic particles are claimed to be suboptimal for effective tumor heating. In contrast, superparamagnetic magnetite nanoparticles were shown to be appropriate for inducing hyperthermia with radiofrequency to Ehrlich tumors (Elsherbini et al., 2011).

No correlation was found between the magnetic moment of a single particle and SPA values for MNPs in the superparamagnetic regime. The optimum particle diameter is suggested to be near the critical size for the single- to multi-domain transition for Fe_3O_4 phase, although the relation between SPA mechanisms and incipient domain walls is still to be determined (Goya et al., 2008).

When using magnetic nanoparticles as a heating source for magnetic particle hyperthermia it is of particular interest to know if the particles are free to move in the interstitial fluid or are fixed to the tumor tissue. The immobilization state determines the relaxation behaviour of the administered particles and thus their specific heating power (Dutz et al., 2011). If the particles are not able to rotate and a temperature increase due to Brown relaxation can be neglected. An investigation showed that carboxymethyl dextran coated magnetic particles are fixed rather strongly to the tumor tissue after injection into a tumor (Dutz et al., 2011).

The effect of Néel relaxation on magnetic nanoparticles unable to move or rotate are studied and losses in linearly and circularly polarized fields are compared (De Châtel et al., 2009). In frequencies lower than the Larmor frequency, linear polarization is found to be the better source of heat power, at high frequencies (beyond the Larmor frequency) circular polarization is preferable. If Néel relaxation in isotropic sample is the dominant mechanism, the technical complications of generating a circularly polarized field in difficult geometry need not be considered.

In order to reach the required temperature with minimum particle concentration in tissue the specific heating power (SHP) of MNP should be as high as possible. The dependence of specific heating power of the size of superparamagnetic particles on the frequency and amplitude of the external alternating magnetic field is found to obey the predictions of relaxation theory. For small mean sizes (about 6 nm) the heating capability is negligibly small whereas larger particles deliver heating suitable for hyperthermia (Glöckl et al., 2006).

Data on SLP commonly reported in the literature show remarkable scattering of the orders of magnitude of 10–100W g^{-1} for a field amplitude of 10 kA m^{-1} and frequency of about 400 kHz (Hergt et al., 2006).

In summary:

1. The SLP of MNP must be considerably increased for achieving useful therapy temperatures in small tumors (at present smaller than 10mm diameter).

2. The main practical problem with MPH is an inadequate MNP supply to the tumor. For IT injection inhomogeneity of MNP distribution in tissue may lead to local temperature differences which do not allow for differentiation of hyperthermia and thermoablation. As a result of insufficient temperature enhancement in parts of the tumor there is a risk of proliferation of surviving tumor cells.

3. For systemic supply of MNP (e.g. antibody targeting) the target enrichment with MNP must be considerably enhanced for achieving therapy temperature. In particular, the therapy of small targets (metastases below presently diagnostic limit) seems to be a questionable hope (Hergt et al., 2007).

The specific loss power useful for hyperthermia is restricted by serious limitations of the alternating field amplitude and frequency. Large values of SLP of the order of some hundreds of W g^{-1} at 400 kHz and 10 kA m^{-1} are found for particles with mean size of about 18 nm provided that the size distribution is sufficiently narrow. A very large value of SLP of nearly 1 kW g^{-1} is found for bacterial magnetosomes having a mean diameter of the magnetite crystals of about 35 nm (Hergt et al., 2006).

MNPs modified with amino silane, which is commonly used in biomedicine, bacterial magnetosomes (BM) exhibit a better heating effect under AMF. Although both particles are found to enhance reduction in cell viability by hyperthermia using MNPs and magnetosomes of the same concentration, current of lower intensity is needed by BMs to produce a similar inhibitory effect in the tumor cell (Liu et al., 2012).

When chains of magnetosomes, which are bound to each other by a filament made of proteins, are incubated in the presence of cancer cells and exposed to an alternating magnetic field of frequency 198 kHz and average magnetic field strength of 20 or 30 mT, they produce efficient inhibition of cancer cell proliferation. This behavior is explained by a high cellular internalization, a good stability in solution and a homogenous distribution of the magnetosome chains, which enables efficient heating (Alphandéry et al., 2012).

When magnetosome chains are heated, the filament binding the magnetosomes together is denatured and individual magnetosomes are obtained which are prone to aggregation, are not stable in solution and do not produce efficient inhibition of cancer cell proliferation under application of an alternating magnetic field (Alphandéry et al., 2012).

Poly(ethylene glycol) methyl ether methacrylate and dimethacrylate with iron oxide as implantable biomaterials. It was demonstrated that the temperature of the hydrogels can be controlled by changing the AMF strength so that the gels either reached hyperthermic (42–45 °C) or thermoablative (60–63 °C) temperatures. The final temperature the hydrogel nanocomposites reach can be tailored to either one of these temperature ranges. The hydrogels were heated in an AMF, and the heating response was shown to be dependent on both iron oxide loading in the gels and the strength of the magnetic field (Meenach et al., 2010).

Cationic magnetoliposome containing both magnetic fluid and the photosensitizer-based complex (CB:ZnPc-ML) were prepared using the thin lipid film method. This result shows that the application of light and AC magnetic field together can be much more effective than the each of the two treatments applied separately (Bolfarini et al., 2012).

Combined effect of magnetic hyperthermia and chemotherapy was evaluated using drug loaded PCPG magnetoliposomes. Thermosensitive drug release took place under the influence of magnetic field and this combined therapy was shown to be more efficient than either treatment alone (Kulshrestha et al., 2012).

It was demonstrated that the temperature achieved with ferromagnetic MNPs was higher than that achieved with superparamagnetic MNPs, even with the same uptake amount into cells. This is due to heating efficiency differences between hysteresis loss and magnetic relaxation. Heat generation predominantly occurs by hysteresis loss rather than by magnetic relaxation. Heat produced by nanoparticles incorporated into cells and adsorbed on cell membranes should be critical for damaging cells, compared with heat produced from outside cells (Baba et al., 2012).

According to some, the well-known iron oxide ferro fluids become undesirable because their iron atoms are poorly distinguishable from those of hemoglobin. A suggested solution is to use mixed-ferrites (MFe_2O_4 where M¼Co, Mn, Ni, Zn) to have a range of magnetic properties. These ferrites have attracted special attention because they save time, and because of their low inherent toxicity, ease of synthesis, physical and chemical stabilities and suitable magnetic properties (Sharifi et al., 2012).

Giri et al. studied citrate coated ferrite particles below 100 nm sizes. Saturation magnetization is found to decrease for coated materials as magnetization is proportional to the amount of weight for the same magnetic material. The coercivity is found to be sufficient for hysteresis loss heating in hyperthermia. The magnetic hysteresis data indicate that these samples (coated) exhibit sufficient hysteresis losses to obtain the temperature required for the destruction of the tumorous cells.

Ferrite particles were prepared in a chitosan matrix at varying ratios (Park et al., 2005). The time period needed for reaching hyperthermia shortened upon increase of chitosan ratio while the saturation magnetization decreases. Optimization of ferrite-chitosan ratio may be promising for hyperthermia applications.

Co-Ti ferrite nanoparticles of 6-12 nm were shown to be suitable for hyperthermia applications (Ichiyanagia et al., 2012). Zn-Gd ferrite particles are suitable but if you cap them with poly (ethylene glycol) PEG, they are not useful (Yao et al., 2009). Co ferrite particles of 7.5 nm copolymerized with poly(methacrylate) and poly(2-hydroxyethylmethacrylate) were shown to be suitable for hyperthermia (Hayashi et al., 2012). $CoFe_2O_4$ ferrite particles (ferromagnetic) were shown to be suitable for hyperthermia (Skumiel, 2006).

Examining the heating produced by nanoparticles of various materials, barium-ferrite and cobalt-ferrite are unable to produce sufficient MFH heating, that from iron-cobalt occurs at a far too rapid rate to be safe, while fcc iron-platinum, magnetite, and maghemite are all capable of producing stable controlled heating. Iron-cobalt MNPs induce temperature changes that are too large, whereas barium-ferrite and cobalt-ferrite MNPs do not provide enough heat to treat a tumor. Simulations showed that magnetite, fcc iron-platinum, and maghemite MNPs are well suited for MFH, making it possible to heat tumors above 41 °C while keeping the surrounding healthy tissue temperatures below this value (Kappiyoor et al., 2010).

The thermoreversible hydrogels (poloxamer, chitosan), which accommodated 20% w/v of the magnetic microparticles, proved to be inadequate. Alginate hydrogels, however, incorporated 10% w/v of the magnetic microparticles, and the external gelation led to strong implants localizing to the tumor periphery, whereas internal gelation failed in situ. The organogel formulations, which consisted of precipitating polymers dissolved in single organic solvents, displayed various microstructures. A 8% poly(ethylene-vinyl alcohol) in DMSO (DMSO: Dimethyl sulfoxide) containing 40% w/v of magnetic microparticles formed the most suitable implants in terms of tumor casting and heat delivery (Le Renard et al., 2010).

Cell culture experiments showed that, by adjusting the amount of magnetic microspheres MMS and the time of exposure to AMF, heat treatments of mild to very high intensities could be achieved using maghemite nanoparticles embedded in mesoporous silica matrix (Martín-Saavedra et al., 2010). The heating effect of iron containing multi walled carbon nanotubes of 10-40 nm were studied and shown to be suitable (Krupskaya et al., 2009).

Several magnetic fluids are shown to be suitable for hyperthermia application. In a comparative study, 16 commercial magnetic fluids are investigated and most suitable ones are distinguished (Kallumadil et al., 2009). Magnetite microcapsules of 20-30 μm embedded in agar phantom exhibited heat generation under an alternating magnetic field (Miyazaki et al., 2012). Magnetite nanoparticles of 10 nm in an aerogel matrix are potential hyperthermia agents where the aerogel matrix can be used for drug loading for combined therapy (Lee et al., 2012).

As can be seen from the aforementioned studies, although there is not a clear definition for an ideal magnetic material for hyperthermia, there are several materials that can be employed, depending on the particular situation. Combined therapies of drug delivery and hyperthermia are promising future outlooks in this field.

Magnetic Drug Carriers

Being potential candidates for drug delivery due to their low toxicity and ability to be targeted, magnetic particles are often coated to stabilize them against precipitation, ensure their low cytotoxicity and to carry the drug in a matrix.

In *in vivo* applications SPION particles should be coated to prevent the drug molecule conjugations and to limit interactions with non-targeted cell sides, to prevent particle agglomeration and for enhanced drug loading and release. Different approaches in SPION coating resulting different assembly of polymers are summarized in Figure 4. In polysaccharide coating and coating with copolymers, the resulted particles are found as uniformly encapsulated cores. In another coating approach, polymer molecules anchored to the magnetic particle surface resulting in a brush like structure. Liposome and micelle forming molecules results a core shell structure with magnetic particles in the core. These structures can be used in drug encapsulation with retaining hydrophobic regions. (Veiseh et al., 2010).
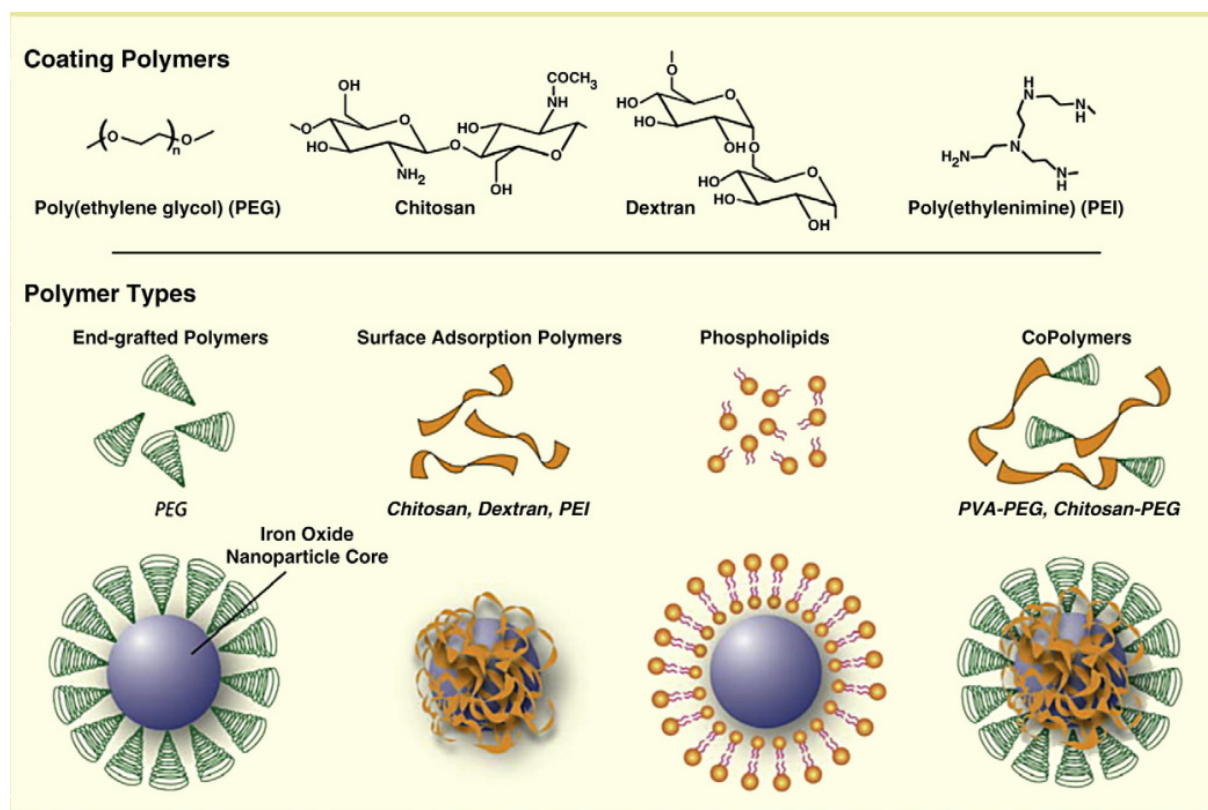
Figure 4. Illustration depicting the assembly of polymers onto the surface of magnetic nanoparticle cores (Veiseh et al., 2010).

Different particles are designed as drug delivery vehicles and a summary of these particles are given in Table 1.

Type of magnetic nanoparticle	Particle size	Coating agent	Drug	Design matrix	Drug release mechanism	Ref
Fe_3O_4	Core diameter of 10 - 15 nm Final diameter of 160 nm	chitosan/PAA multilayer	cefradine	Layer-by-Layer (LBL) The drug molecules were entrapped inside the hollow spheres through diffusion process	pH responsive	Zhang et al., 2006
Fe_3O_4	Final diameter of >1 μm	sodium carboxy methyl cellulose and chitosan	------	self-assembly shell composed of layers of carboxy methyl cellulose and chitosan around the magnetic core	------------	Cui et al., 2011
Fe_3O_4	Core diameter of 8 nm Final diameter of of 107 nm	chitosan	cefradine	cross-linking the particles with glutaraldehyde and the drug is embedded in the polymer matrix	pH responsive	Li et al., 2007
Fe_3O_4	Core diameter of 5 nm Final diameter of 1–1.5cm	Alginate / chitosan	insulin	insulin encapsulation in alginate/chitosan beads. The beads containing insulin were prepared in triplicate by extrusion method.	Magnetic field	Finotelli et al., 2010

Type of magnetic nanoparticle	Particle size	Coating agent	Drug	Design matrix	Drug release mechanism	Ref
Fe_3O_4	Final diameter of 200 nm	multiwalled carbon nanotubes (MWNTs)	doxorubicin	The MWNT-hybrid nanocomposites provided an efficient way for the extraction and enrichment of doxorubicin via π–π stacking of DOX molecules onto the polyaromatic surface of MWNTs.	pH responsive	Shen et al., 2011
Fe_3O_4	Core diameter of 3 nm	CNTs	---------	Magnetic nanoparticles adsorb on the CNT ends	------	Panczyk et al., 2010
Fe_3O_4	Core diameter of 5–10 nm. CNTs average diameter of about 30–50 nm and average length of about 100–500 nm	CdTe QDs and CNTs	-------	CNT-SPIO-CdTe nanohybrids via LBL assembly	----------	Chen et al., 2010
$γ-Fe_2O_3$	Core diameter of 10 nm	CNT	Diaminophenothiazine (methylene blue)	monodisperse, inherently open-ended, multi-wall CNTs loaded with magnetic iron-based nanoparticles that are encapsulated within the tube graphitic walls		Vermisoglou et al., 2011
Fe_3O_4	Core diameter of 8–12 nm mACs had a mean diameter of about 30 nm MWNTs= 40-60 nm	(mMWNTs) and magnetic-activated carbon particles (mACs)	gemcitabine (GEM)	Fe_3O_4 nanoparticles are on the outer surface of the PAA functionalized MWNTs and the drug is adsorbed on the surface .		Yang et al., 2011
$CoFe_2O_4$ nanoparticles	Core diameter of 6 nm MWCNTs with an outer diameter of 10–30 nm and an average length of 0.5–2 μm	MWCNT/cobalt ferrite ($CoFe_2O_4$) magnetic hybrids	doxorubicin	cobalt ferrite is on the outer surface of the MWCNT	pH responsive	Wu et al., 2011
$γ-Fe_2O_3$	Core diameter of 5 nm Final diameter of 100 nm	DNA	fluorescein	Single-stranded DNA was immobilized onto the silica network, and the magnetic particles are loaded onto the network. The complementary DNA sequence was then attached to magnetic nanoparticles.	Temperature responsive	Ruiz-Hernandez et al., 2011

Type of magnetic nanoparticle	Particle size	Coating agent	Drug	Design matrix	Drug release mechanism	Ref
Fe_3O_4	Core diameter of of 8 nm Final diameter of 150 nm	PEG-functionalized porous silica shell	doxorubi-cin	DOZ conjugated magnetite particles are coated with silica to obtain core/shell nanoparticles and the whole composite is coated with PEG	the breaking of the bonding of the drug to the carrier or the swelling and degradation of the polymer.	Chen et al., 2010
α-Fe_2O_3	Core diameter of 13 nm micron-sized mesoporous molecular sieves (with 2.9-nm pores) MCM-41 and MCM-48 powders gave mean pore sizes of 3.7 and 3.5 nm, a size between 1 and 4 μm. and hollow silica microcapsules (pores of 2.7, average diameter being around 3 μm. and 15 nm. 250-nm wall thickness	hollow silica microcapsules	---------	Magnetic particles are encapsulated inside the hollow silica microcapsules	------------	Arruebo et al., 2006
Fe_3O_4	Core diameter of 10 nm Final diameter of 100 nm with 20 nm silica shell	SiO_2@ Fe_3O_4 core–shell NPs		Silica-magnetite nanocomposites are emulsified and self-assembly of magnetic-mesoporous heteronanorods at the interface of water-in-oil droplets takes place.		Zhang et al., 2011
Fe_3O_4	Particles between 150nm and 4.5 μm	silica,arabic acid and cross-linked polysaccharide	antibody	particles with starch derivative or polymeric arabic acid as matrix material functionalized with an antibody	---	Sieben et al., 2001
Fe_3O_4	Final diameter if 202 nm	β-cyclodextrin and pluronic polymer (F-127)	curcumin	multi-layer polymer coating around the magnetic particle and the drug is encapsulated via diffusion into polymer matrix	The initial burst of release was due to immediate dissociation of surface bound curcumin molecules that	Yallapu et al., 2011

Type of magnetic nanoparticle	Particle size	Coating agent	Drug	Design matrix	Drug release mechanism	Ref
					exist on the CD or F127 polymer matrix. The remaining sustained drug release was due to the slow release of the drug entrapped inside CD and/or F127 polymer layers.	
Fe_3O_4	Core diameter of 14.8 nm	2-hydroxypropyl-cyclodextrin (HCD) onto the gum arabic modified magnetic nanoparticles (GAMNP)	ketoprofen	polymers grafted onto magnetic particles(Multilayer polymer matrix)	drug molecules are rapidly released from HCDGAMNP, whereas some remains associated to degredation of HCD-GAMNP	Banerjee & Chen, 2009
Fe_3O_4	Final diameter of 13 nm.	(3-aminopropyl) triethoxysilane coated (APTES-MNPs) with b-cyclodextrin (β-CD).	-------	layer-by-layer	---------	Cao et al., 2009
Fe_3O_4	Core diameter of 9.2 nm	Oleic acid, sodium dodecyl benzene sulfonate SDBS, bovine serum albumin (BSA)	---	Oleic acid capped magnetic nanoparticles are embedded in the SDBS micelle and BSA adsorbs onto the micellar entity.	----	Yang et al., 2009
Fe_3O_4	Final diameter of 300 nm	poly (N-isopropylacrylamide) PNIPAAm and poly(D,L-lactide-co-glycolide) PLGA	Bovine serum albumin (BSA) and curcumin	(MLNPs) with a magnetic core and two shells made up of temperature-sensitive polymers (PNIPAAm) were encapsulated with PLGA. BSA was first loaded into PNIPAAm magnetic nanoparticles. Second, curcumin was loaded to PLGA to form the multilayer nanoparticles	Temperature responsive	Koppolu et al., 2010
Fe_3O_4	Final diameter of 150 nm	dextran	fluorescein (Fluo) or TEXAS RED® (Texas) fluorescent dye	By oxidizing Ferumoxides (FE) (suspension consisting of dextran- coated SPION) hydroxyl groups on the dextran coating are oxidized to aldehyde groups. Lysine fixable fluorescein (Fluo) or TEXAS RED® (Texas) fluorescent dye (supplied as lysine fixable dextran conjugates) was reacted with aldehyde FE and the fluorescent dye is conjugated to FE SPION (FL FE).	----	Lee et al., 2008

Type of magnetic nanoparticle	Particle size	Coating agent	Drug	Design matrix	Drug release mechanism	Ref
Fe_3O_4	Core diameter of 5 5 nm Final diameter of 4 μm,	Fe_3O_4/ PAH	fluorescein isothiocyanate (FITC)-Dextran	layer-by-layer (LbL) assembly FITC-dextran nanoparticle is coated with PSS polyelectrolyte which contains the magnetic particles forming a magnetic shell around the particle.	Magnetic field	Hu et al., 2008
Fe_3O_4	Core diameter of 12 nm	coated with starch, dextran, PEG or MPEG	----	Polymeric networks cover a large number of continuous magnetic monodomains.	----	Huong et al., 2009
magnetic fluids Carboxyde-xtran coated DDM128 P6 (dextran–magnetite) Aminosilane coated (aminosilane–magnetite) MFL AS	DDM128 P6: core diameter of 3 nm MFL AS: core diameter of 15 nm.	dextran- or aminosilane-coated	----		-----	Jordan et al., 2006
Fe_3O_4	Core diameter of 7 nm	PVA and starch		PVA coated particles as large clusters where starch coated ones are be densely dispersed in the polymeric matrix		Voit et al., 2001
Fe_3O_4	Final diameter of 110±22 nm	starch	------	Core-shell particles	-----	Chertok et al., 2008
Fe_3O_4	coated with starch (G100) particles final diameter of 110 (±22) nm gumarabic polysaccharide Matrix (Gara) particles final diameter of 189nm Final diameter 225 nm after PEI addition	Polyethyleneimine (PEI)	--------	Surface modification of carboxyl-bearing Gara nano particles with PEI	--------	Chertok et al., 2010
Fe_3O_4	Final diameter of (140-190 nm)	Aminated, cross-linked starch and aminosilane coated Fe_3O_4 modified with PEG		To ensure that cross-linked starch particles was functionally similar to aminosilane coated particles, starch particles were covalently strengthened and aminated with concentrated ammonia to form aminated-precursor (DN). PEG is then linked to aminated precursors, DN and aminosilane particles with N-Hydroxysuccinimide (NHS) chemistry.		Cole et al., 2011

Type of magnetic nanoparticle	Particle size	Coating agent	Drug	Design matrix	Drug release mechanism	Ref
Fe_3O_4	Core diameter of 4-10 nm	PVA and PVA with partially exchanged carboxyl groups.	----		-----	Lee et al., 1996
Fe_3O_4	Core diameter of 10 nm	PVA matrix	---	the films of 200 mm depth and different concentrations of iron oxide particles in the PVA matrix.	----	Novakova et al., 2003
Fe_3O_4	Core diameter of 5–10 nm Final diameter of 108-155 nm	PVA	----	core-shell, all iron-oxide particles surrounded by a layer of PVA polymer.	----	Qui & Winnik, 2000
$\gamma\text{-}Fe_2O_3$	Core diameter of 14, 19 and 43 nm Final particles are of diameter 43 nm	PNIPAM	doxorubicin	MNP cluster is coated with PNIPAM and the nanoparticl is dehydrated. Core shell morphology is achieved with dispersion free-radical polymerization	Thermoresponsive	Purushotham et al., 2009
Fe_3O_4	core diameter of 13 nm	PNIPAM	doxorubicin	Core shell morphology by dispersion polymerization where drug loaded PNIPAM shell contains magnetite clusters.	Thermoresponsive	Purushotham et al., 2010
Fe_3O_4	Core diameter of 11.21 nm Final particles are of diameter less than 250 μm	PMMA	fluorescein isothiocyanate (FITC)		Thermoresponsive	Urbina et al., 2008
$\gamma\text{-}Fe_2O_3$	Core diameter of 20 nm Final particles are of diameter 400 nm	carbon	doxorubicin	Drug is released form the surface of on-coated or partially coated magnetic particles	released from the surface of our particles at a slow rate via desorption	Ibarra et al., 2007
Fe_3O_4	Final particles are of diameter ~10-20 nm	poly[aniline-co-sodium N-(1-onebutyric acid)] aniline (SPAnNa)	1,3-bis(2-chloroethyl)-1-nitrosourea	Microcapsule nanoparticles are encapsulated during the aggregation, forming the Fe_3O_4/SPAnH nanoparticles	Ultrasound and externally applied magnetic field.	Chen et al., 2010
Fe_3O_4	Core diameter of 8 nm Final particles of diameter 5.2 μm	PEs: poly(styrene sulfonate) (PSS, Mw~70000) and poly(allylamine hydrochloride) (PAH, Mw~50000).		Melamine formaldehyde microparticle is coated with polyelectrolytes (PE) in a layer-by-layer (LbL) assembly by solvent controlled precipitation of PE. The core is then dissolved and nanoparticles are infiltrated into the capsule core.		Gaponik et al., 2004
Fe_3O_4	Final particle diameter of 300–1300 nm	polystyrene		Similar technique to abovementioned method.		Madani et al., 2011

Type of magnetic nanoparticle	Particle size	Coating agent	Drug	Design matrix	Drug release mechanism	Ref
Fe_3O_4	Core diameter of 13 nm Final particle diameter of 3 μm	poly(sodium 4-styrenesulfonate) (PSS) and poly(allylamine hydrochloride) (PAH)	Dye	Similar technique to abovementioned method.	Magnetic heating	Katagiri et al., 2010
Fe_3O_4	Core diameter of 20 nm Final particle diameter of 2.82 μm	(PDDA/PSS)2/PDDA	Dye	Similar technique to abovementioned method.	Magnetic heating	Katagiri et al., 2011
Fe_3O_4 and γ-Fe_2O_3	Fe_3O_4 and γ-Fe_2O_3 core diameters of 9.5 and 4.3 nm, respectively	Ca alginate beads	-----	The nanoparticles were entrapped in Ca alginate beads, "egg-box like" structure of Ca alginate	-------	Finotelli et al., 2005
Fe_3O_4	Particle diameter of 58 nm	NP aggregates in humic acid (HA)	---	HA adsorbs onto magnetite particles	------	Hu et al., 2010
Fe_3O_4	Final particle diameter of 7.5 nm	amino silane(3-aminopropyl triethoxysilane)	---	nearly monolayer coating of amino silane on the magnetite particle surface	---	Ma et al., 2003
Fe_3O_4	Core particle diameter of 10–15 nm Final particle diameter of 400±80 nm	poly-L-lysine hydrochloride (PLL), poly-L-glutamic acid (PGA)	DNA	layer-by-layer (LbL) assembly on polycarbonate templates with subsequent removal of these templates. In the inner surface of polycarbonate templates, first poly-L-lysine hydrochloride (PLL) and poly-L-glutamic acid (PGA) are absorbed linking by electrostatic interactions as a polyelectrolyte layer. Then, multi polyelectrolyte layers are assembled on polycarbonate membrane and Fe_3O_4 nanoparticles are linked to PLL layer as Fe_3O_4/PLL bilayers.	-----------	He et al., 2008
γ-Fe_2O_3	Core diameters of 12 nm. Final particle diameter of 35 nm (PEI) and 46 nm (PEI plus PEO-PGA)	Poly(ethylene imine) and Poly(ethylene oxide)-block-poly(glutamic acid)	---	MNPs stabilized with polymers in two layer-by-layer deposition steps.	----	Thunemann et al., 2006
Fe_3O_4	Core diameter of 12 nm	aminosilane coating	---	----	---	Maier-Hauff et al., 2011

Type of magnetic nanoparticle	Particle size	Coating agent	Drug	Design matrix	Drug release mechanism	Ref
Fe_3O_4 and γ-Fe_2O_3	Core diameters of 10 nm Final particle diameter of 96 ±15 nm	poly(ethylene glycol) (PEG)	doxorubicin	one-pot synthesis of colloids of SPION-DOX-PEG particles, PEG shell reduces the access of cellular enzymes to the drug-particle linkage and thus limits and/or delays the anticancer effect.	specific release mechanism for drug delivery is enzymatic cleavage, however the PEG shell seems to reduce the access of cellular enzymes to the drug-particle linkage and thus limits and/or delays the anticancer effect.	Shkilnyy et al., 2010

Table 1. Summary of magnetic nanomaterials used in drug delivery.

5. Conclusion

In this review, uses of magnetic nanoparticles in drug delivery are summarized. Magnetic nanoparticles gained a lot of interest due to their biocompatibility, low toxicity and their ability to be manipulated upon application of a magnetic field. These special properties allow them to be utilized as drug carrier vehicles, either by direct attachment of the drug onto the particle or often by using a natural or synthetic polymer to aid carry the drug and embedding the magnetic particles in the polymer matrix. Several types of drugs and coatings have been explored as drug carriers and a very limited selection is summarized in Table 1. The ease of surface modification of these particles opens the opportunity for targeting moieties to be attached onto particle surface, facilitating the targeting. Targeting with magnetic nanoparticles is predominantly carried out upon application of an external magnetic field, which act as an external force to localize the particles in the desired areas in the body. Applying an alternating magnetic field to magnetic particles once they are in the vicinity of a tumor, results in the temperature of the medium to rise up to 42 ºC, which is the temperature required for hyperthermia, a complementary treatment along with chemotherapy and radiotherapy. We believe that these fascinating particles will find further potential applications along with more success in the present ones in the very near future.

Author details

Seyda Bucak and Banu Yavuztürk
Yeditepe University, Istanbul, Turkey

Ali Demir Sezer
Marmara University, Istanbul, Turkey

6. References

Alexiou, C.; Tietze, R.; Schreiber, E.; Jurgons, R.; Richter, H.; Trahms, L.; Rahn, H.; Odenbach, S. & Lyer, S. (2011). Cancer therapy with drug loaded magnetic nanoparticles—magnetic drug targeting, Journal of Magnetism and Magnetic Materials, Vol.323, pp.1404-1407.

Alphandéry, E.; Guyot, F. & Chebbi, I. (2012). Preparation of chains of magnetosomes, isolated from Magnetospirillum magneticum strain AMB-1 magnetotactic bacteria, yielding efficient treatment of tumors using magnetic hyperthermia, International Journal of Pharmaceutics, Vol.434, pp.444-452.

Arruebo, M.; Galan, M.; Navascues, N.; Tellez, C.; Marquina, C.; Ibarra, M.R. & Santamaria, J. (2006). Development of Magnetic Nanostructured Silica-Based Materials as Potential Vectors for Drug-Delivery Applications, Chemistry of Materials, Vol.18, pp.1911-1919.

Auffan, M.; Decome, L.; Ros,e J.; Orsiere, T.; De Meo, M. & Briois, V. (2006). *In vitro* interactions between DMSA-coated maghemite nanoparticles and human fibroblasts: a physicochemical and cyto-genotoxical study, Environmental Science & Technology, Vol.40, pp.4367-4373.

Baba, D.; Seiko, Y.; Nakanishi, T.; Zhang, H.; Arakaki, A.; Matsunaga, T. & Osaka, T. (2012). Effect of magnetite nanoparticles on living rate of MCF-7 human breast cancer cells, Colloids Surf B Biointerfaces, Vol.95, pp.254-257.

Bae, J.-E.; Huh, M.-I.; Ryu, B.-K.; Do, J.-Y.; Jin, S.-U.; Moon, M.-J.; Jung, J.-C.; Chang, Y.; Kim, E.; Chi, S.-G.; Lee, G.-H. & Chae, K.-S. (2011). The effect of static magnetic fields on the aggregation and cytotoxicity of magnetic nanoparticles, Biomaterials, Vol.32, pp.9401-9414.

Banerjee, S.S. & Chen D.-H. (2009). Cyclodextrin-conjugated nanocarrier for magnetically guided delivery of hydrophobic drugs, Journal of Nanoparticle Research, Vol.11, pp.2071-2078.

Berry, C.C.; Wells, S.; Charles, S. & Curtis, A.S. (2003). Dextran and albumin derivatised iron oxide nanoparticles: influence on fibroblasts *in vitro*, Biomaterials, Vol.24, pp.455-457.

Bolfarini, G.C.; Siqueira-Moura, M.P.; Demets, G.J.F.; Morais, P.C. & Tedesco, A.C. (2012). *In vitro* evaluation of combined hyperthermia and photodynamic effects using magnetoliposomes loaded with cucurbit[7]uril zinc phthalocyanine complex on melanoma, Journal of Photochemistry and Photobiology B: Biology, DOI:10.1016/j.jphotobiol.2012.05.009, impress.

Cao, H.; He, J.; Deng, L. & Gao, X. (2009). Fabrication of cyclodextrin-functionalized superparamagnetic Fe_3O_4/amino-silane core–shell nanoparticles via layer-by-layer method, Applied Surface Science, Vol.255, pp.7974-7980.

Caruntu, D.; Caruntu, G. & O'Connor, C.J. (2007). Magnetic properties of variable-sized Fe3O4 nanoparticles synthesized from non-aqueous homogeneous solutions of polyols, Journal of Physics D: Applied Physics, Vol.40, pp.5801-5809.

Chan, W.C.W.; Maxwell, D.J.; Gao, X.H.; Bailey, R.E.; Han, M.Y. & Nie, S.M. (2002). Luminescent QDs for multiplexed biological detection and imaging, Current Opinion in Biotechnology, Vol.13, pp.40-46.

Chang, E.; Alexander, H.R.; Libutti, S.K.; Hurst, R.; Zhai, S.; Figg, W.D. & Bartlett, D.L. (2001). Laparoscopic continuous hyperthermic peritoneal perfusion, Journal of the American College of Surgeons, Vol.193, pp.225–229.

Chen, A.-Z.; Lin, X.-F.; Wang, S.-B.; Li, L.; Liu, Y.-G.; Ye, L. & Wang, G.-Y. (2012). Biological evaluation of Fe3O4–poly(l-lactide)–poly(ethylene glycol)–poly(l-lactide) magnetic microspheres prepared in supercritical CO2, Toxicology Letters, Vol.212, pp.75-82.

Chen, B.; Zhang, H.; Zhai, C.; Du, N.; Sun, C.; Xue, J.; Yang, D.; Huang, H.; Zhang, B.; Xiec, Q. & Wu Y. (2010). Carbon nanotube-based magnetic-fluorescent nanohybrids as highly efficient contrast agents for multimodal cellular imaging, Journal of Materials Chemistry, Vol.20, pp.9895-9902.

Chen, D.; Jiang, M.; Li, N.; Gu, H.; Xu, Q.; Ge, J.; Xia, X. & Lu, J. (2010). Modification of magnetic silica/iron oxide nanocomposites with fluorescent polymethacrylic acid for cancer targeting and drug delivery, Journal of Materials Chemistry, Vol.20, pp.6422-6429.

Chen, F.-H.; Zhang, L.-M.; Chen, Q.-T.; Zhang, Y. & Zhang, Z.-J. (2010). Synthesis of a novel magnetic drug delivery system composed of doxorubicin-conjugated Fe3O4 nanoparticle cores and a PEG-functionalized porous silica Shell, Chemical Communications, Vol.46, pp.8633-8635.

Chen, P.-Y.; Liu, H.-L.; Hua, M.-Y.; Yang, H.-W.; Huang, C.-Y.; Chu, P.-C.; Lyu, L.-A.; Tseng, I-C.; Feng, L.-Y.; Tsai, H.-C.; Chen, S.-M.; Lu, Y.-J.; Wang, J.-J.; Yen, T.-C.; Ma, Y.-H.; Wu, T.; Chen, J.-P.; Chuang, J.-I.; Shin, J.-W.; Hsueh, C. & Wei, K.-C. (2010). Novel magnetic/ultrasound focusing system enhances nanoparticle drug delivery for glioma treatment, Neuro-Oncology, Vol.12, pp.1050-1060.

Chertok, B.; David, A.E. & Yang, V.C. (2010). Polyethyleneimine-modified iron oxide nanoparticles for brain tumor drug delivery using magnetic targeting and intra-carotid administration, Biomaterials, Vol.31, pp.6317-6324.

Chertok, B.; Moffat, B.A.; David, A.E.; Yu, F.; Bergemann, C.; Ross, B.D. & Yang, V.C. (2008). Iron Oxide Nanoparticles as a Drug Delivery Vehicle for MRI Monitored Magnetic Targeting of Brain Tumors, Biomaterials, Vol.29, pp.487-496.

Cole, A.J.; David, A.E.; Wang, J.; Galbán, C.J.; Hill, H.L. & Yang, V.C. (2011). Polyethylene glycol modified, cross-linked starch-coated iron oxide nanoparticles for enhanced magnetic tumor targeting, Biomaterials, Vol.32, pp.2183-2193.

Cole, A.J.; David, A.E.; Wang, J.; Galbán, C.J. & Yang, V.C. (2011). Magnetic brain tumor targeting and biodistribution of long-circulating PEG-modified, cross-linked starch-coated iron oxide nanoparticles, Biomaterials, Vol.32, pp.6291-6301.

Cole, A.J.; Yang, V.C. & David, A.E. (2011). Cancer theranostics: the rise of targeted magnetic nanoparticles, Trends in Biotechnology, Vol. 29, pp. 323-332.

Cui, M.; Wang, F.-J.; Shao, Z.-Q.; Lu, F.-S. & Wang, W.-J. (2011). Influence of DS of CMC on morphology and performance of magnetic microcapsules, Cellulose, Vol.18, pp.1265-1271.

De Châtel, P.F.; Nándori, I.; Hakl, J.; Mészáros, S. & Vad, K. (2009). Magnetic particle hyperthermia: Néel relaxation in magnetic nanoparticles under circularly polarized field, Journal of Physics: Condensed Matter, Vol.21, pp.124202-10.

Ding, J.; Tao, K.; Li, J.; Song, S. & Sun K. (2010). Cell-specific cytotoxicity of dextran-stabilized magnetite nanoparticles, Colloids and Surfaces B: Biointerfaces, Vol.79, pp.184–190.

Ding, G.; Guo, Y.; Lv, Y.; Liu, X.; Xu, L. & Zhang, X. (2012). A double-targeted magnetic nanocarrier with potential application in hydrophobic drug delivery, Colloids and Surfaces B: Biointerfaces, Vol.91, pp.68-76.

Dutz, S.; Kettering, M.; Hilger, I.; Müller, R. & Zeisberger, M. (2011). Magnetic multicore nanoparticles for hyperthermia--influence of particle immobilization in tumor tissue on magnetic properties, Nanotechnology, Vol.22, pp.265102-09.

Elsherbini, A.A.; Saber, M.; Aggag, M.; El-Shahawy, A. & Shokier, H.A. (2011). Magnetic nanoparticle-induced hyperthermia treatment under magnetic resonance imaging, Magnetic Resonance Imaging, Vol.29, pp.272–280.

Falk, M.H. & Issels, R.D. (2001). Hyperthermia in oncology, International Journal of Hyperthermia, Vol.17, pp.1–18.

Feldman, A.L.; Libutti, S.K.; Pingpank, J.F.; Bartlett, D.L.; Beresnev, T.H.; Mavroukakis, S.M.; Steinberg, S.M.; Liewehr, D.J.; Kleiner, D.E. & Alexander, H.R. (2003). Analysis of Factors Associated with Outcome in Patients with Malignant Peritoneal Mesothelioma Undergoing Surgical Debulking and Intraperitoneal Chemotherapy, Journal of Clinical Oncology, Vol.21, pp.4560-4567.

Finotelli, P.V.; Da Silva, D.; Sola-Penna, M.; Rossi, A.M.; Farina, M.; Andrade, L.R.; Takeuchi, A.Y. & Rocha-Leao, M.H. (2010). Microcapsules of alginate/chitosan containing magnetic nanoparticles for controlled release of insulin, Colloids and Surfaces B: Biointerfaces, Vol.81, pp.206-211.

Finotelli, P.V.; Sampaio, D.A.; Morales, M.A.; Rossi, A.M. & Rocha-Leão, M.H. (2005). Ca Alginate as Scaffold for Iron Oxide Nanoparticles Synthesis, 2nd Mercosur Congress on Chemical Engineering, 4th Mercosur Congress on Process Systems Engineering, Rio de Janeiro – Brazil.

Forbes, Z.G.; Yellen, B.B.; Barbee, K.A. & Friedman, G. (2003). An Approach to Targeted Drug Delivery Based on Uniform Magnetic Fields, IEEE Transactions on Magnetics, Vol.39, pp.3372-3377.

Gaponik, N.; Radtchenko, I.L.; Sukhorukov, G.B. & Rogach, A. L. (2004). Luminescent Polymer Microcapsules Addressable by a Magnetic Field, Langmuir, Vol.20, pp.1449-1452.

Gitter, K. & Odenbach, S. (2011). Experimental investigations on a branched tube model in magnetic drug targeting, Journal of Magnetism and Magnetic Materials, Vol. 323, pp.1413-1416.

Gitter, K. & Odenbach, S. (2011). Quantitative targeting maps based on experimental investigations for a branched tube model in magnetic drug targeting, Journal of Magnetism and Magnetic Materials, Vol.323, pp.3038-3042.

Glöckl, G.; Hergt, R.; Zeisberger, M.; Dutz, S.; Nagel, S. & Weitschies, W. (2006). The effect of field parameters, nanoparticle properties and immobilization on the specific heating power in magnetic particle hyperthermia, Journal of Physics: Condensed Matter, Vol.18, pp.S2935-S2949.

Gonzales-Weimuller, M.; Zeisberger, M. & Krishnan, K.M. (2009). Size-dependant heating rates of ironoxide nanoparticles for magnetic fluid hyperthermia, Journal of Magnetism and Magnetic Materials, Vol.321, pp.1947-1950.

Goya, G.F.; Lima, E.; Jr.; Arelaro, A.D.; Torres, T.; Rechenberg, H.R.; Rossi, L.; Marquina, C. & Ibarra, M.R. (2008). Magnetic Hyperthermia with Fe3O4 Nanoparticles: The Influence of Particle Size on Energy Absorption, IEEE Transactions on Magnetics, Vol.44, pp.4444-4447.

Häfeli, U.A.; Riffle, J.S.; Carmichael-Baranauskas, A.; Harris-Shekhawat, L.; Mark, F.; Dailey, J.P. & Bardenstein, D. (2009) Cell Uptake and *in vitro* Toxicity of Magnetic Nanoparticles Suitable for Drug Delivery, Molecular Pharmaceutics, Vol.6, pp.1417-1428.

Hayashi, K.; Maeda, K.; Moriya, M.; Sakamoto, W. & Yogo, T. (2012). In situ synthesis of cobalt ferrite nanoparticle / polymer hybrid from a mixed Fe–Co methacrylate for magnetic hyperthermia, Journal of Magnetism and Magnetic Materials, Vol.324, pp.3158-3164.

He, Q.; Tian, Y.; Cui, Y.; Möhwald H. & Li, J. (2008). Layer-by-layer assembly of magnetic polypeptide nanotubes as a DNA carrier, Journal of Materials Chemistry, Vol.18, pp.748-754.

Hergt, R. & Dutz, S. (2007). Magnetic particle hyperthermia—biophysical limitations of a visionary tumor therapy, Journal of Magnetism and Magnetic Materials, Vol.311, pp.187-192.

Hergt, R.; Dutz, S.; Müller, R. & Zeisberger, M. (2006). Magnetic particle hyperthermia: nanoparticle magnetism and materials development for cancer therapy, Journal of Physics: Condensed Matter, Vol.18, pp.S2919-S2934.

Hu, J.-D.; Zevi, Y.; Kou, X.-M.; Xiao, J.; Wang, X.-J. & Jin, Y. (2010). Effect of dissolved organic matter on the stability of magnetite nanoparticles under different pH and ionic strength conditions, Science of the Total Environment, Vol.408, pp.3477-3489.

Hu, S.-H.; Tsai, C.-H.; Liao, C.-F.; Liu, D.-M. & Chen, S.-Y. (2008). Controlled Rupture of Magnetic Polyelectrolyte Microcapsules for Drug Delivery, Langmuir, Vol.24, pp.11811-11818.

Hua, M.-Y.; Liu, H.-L.; Yang, H.-W.; Chen, P.-Y.; Tsai, R.-Y.; Huang, C.-Y.; Tseng, I.-C.; Lyu, L.-A.; Ma, C.-C.; Tang, H.-J.; Yen, T.-C. & Wei, K.-C. (2011). The effectiveness of a magnetic nanoparticle-based delivery system for BCNU in the treatment of gliomas, Biomaterials, Vol.32, pp.516-527.

Hua, M.Y.; Yang, H.W.; Liu, H.L.; Tsai, R.Y; Pang, S.T.; Chuang, K.L.; Chang, Y.S.; Hwang, T.L.; Chang Y.H.; Chuang, H.C. & Chuang, C.K. (2011). Superhigh-magnetization nanocarrier as a doxorubicin delivery platform for magnetic targeting therapy, Biomaterials, Vol.32, pp.8999-9010.

Huang, C.; Tang, Z.; Zhou, Y.; Zhou, X.; Jin, Y.; Li, D.; Yang, Y. & Zhou, S. (2012). Magnetic micelles as a potential platform for dual targeted drug delivery in cancer therapy, International Journal of Pharmaceutics, Vol.429, pp.113-22.

Huong, N.T.; Giang, L.T.K.; Binh, N.T. & Minh, L.Q. (2009). Surface modification of iron oxide nanoparticles and their conjunction with water soluble polymers for biomedical application, Journal of Physics: Conference Series, Vol.187, pp.012046-51.

Ibarra, M.R.; Fernandez-Pacheco, R.; Valdivia, J.G.; Marquina C. & Gutierrez, M. (2007). Magnetic Nanoparticle Complexes for Drug Delivery, and Implanted Magnets for Targeting, American Institute of Physics, Vol.898, pp.99-105.

Ichiyanagia, Y.; Shigeoka, D.; Hiroki, T.; Mashino, T.; Kimura, S.; Tomitaka, A.; Ueda, K. & Takemura, Y. (2012). Study on increase in temperature of Co–Ti ferrite nanoparticles for magnetic hyperthermia treatment, Thermochimica Acta, Vol.532, pp.123–126.

Jordan, A.; Scholz, R.; Maier-Hauff, K.; van Landeghem, F.K.H.; Waldoefner, N.; Teichgraeber, U.; Pinkernelle, J.; Bruhn, H.; Neumann, F.; Thiesen, B.; von Deimling, A. & Felix, R. (2006). The effect of thermotherapy using magnetic nanoparticles on rat malignant glioma, Journal of Neuro-Oncology, Vol.78, pp.7-14.

Jordan, A.; Wust, P.; Fähling, H;. John, W.; Hinz, A. & Felix, R. (1993). Inductive heating of ferrimagnetic particles and magnetic fluids: physical evaluation of their potential for hyperthermia, International Journal of Hyperthermia, Vol.9, pp.51-68.

Jung, C.W. & Jacobs, P. (1995). Physical and chemical properties of superparamagnetic iron oxide MR contrast agents: ferumoxides, ferumoxtran, ferumoxsil, Magnetic Resonance Imaging, Vol.13, pp.661-674.

Kallumadil, M.; Tada, M.; Nakagawa, T.; Abe, M.; Southern P. & Pankhurst, Q.A. (2009). Suitability of commercial colloids for magnetic hyperthermia, Journal of Magnetism and Magnetic Materials, Vol. 321, pp. 1509-1513.

Kappiyoor, R.; Liangruksa, M.; Ganguly, R. & Puri, I.K. (2010). The effects of magnetic nanoparticle properties on magnetic fluid Hyperthermia, Journal of Applied Physics, Vol.108, pp.094702-8.

Karlsson, H.L.; Cronholm, P.; Gustafsson, J. & Moller, L. (2008). Copper oxide nanoparticles are highly toxic: a comparison between metal oxide nanoparticles and carbon nanotubes, Chemical Research in Toxicology, Vol.21, pp.1726-1732.

Karlsson, H.L.; Gustafsson, J.; Cronholm, P. & Moller L. (2009). Size dependent toxicity of metal oxide particles--a comparison between nano- and micrometer size, Toxicology Letters, Vol.188, pp. 112-118.

Katagiri, K.; Imai, Y. & Koumoto, K. (2011). Variable on-demand release function of magnetoresponsive hybrid capsules, Journal of Colloid and Interface Science, Vol.361, pp.109-114.

Katagiri, K.; Nakamura, M. & Koumoto, K. (2010). Magnetoresponsive Smart Capsules Formed with Polyelectrolytes, Lipid Bilayers and Magnetic Nanoparticles, American Chemical Society, Vol. 2, pp.768-773.

Koppolu, B.; Rahimi, M.; Nattama, S.; Wadajkar, A. & Nguyen, K.T. (2010). Development of multiple-layer polymeric particles for targeted and controlled drug delivery, Nanomedicine: Nanotechnology, Biology, and Medicine, Vol.6 pp.355-361.

Krukemeyer, M.G.; Krenn, V.; Jakobs, M. & Wagner, W. (2012). Mitoxantrone-iron oxide biodistribution in blood, tumor, spleen and liver—magnetic nanoparticles in cancer treatment, Journal of Surgical Research, Vol.175, pp.35-43.

Krupskaya, Y.; Mahn, C.; Parameswaran, A.; Taylor, A.; Kramer, K.; Hampel, S.; Leonhardt, A.; Ritschel, M.; Büchner, B. & Klingeler, R. (2009). Magnetic study of iron-containing

carbonnanotubes: Feasibility for Magnetic hyperthermia, Journal of Magnetism and Magnetic Materials, Vol.321, pp.4067-4071.

Kulshrestha, P.; Gogoa, M.; Bahadur, D. & Banerjee, R. (2012). *In vitro* application of paclitaxel loaded magnetoliposomes for combined chemotherapy and hyperthermia, Colloids and Surfaces B: Biointerfaces, Vol.96, pp.1-7.

Kumar, C.S.S.R. & Mohammad, F. (2011). Magnetic nanomaterials for hyperthermia-based therapy and controlled drug delivery, Advanced Drug Delivery Reviews, Vol.63, pp.789–808.

Kuznetsov, O.A.; Brusentsov, N.A.; Kuznetsov, A.A.; Yurchenko, N.Y.; Osipov, N.E. & Bayburtskiy, F.S. (1999). Correlation of the coagulation rates and toxicity of biocompatible ferromagnetic microparticles, Journal of Magnetism and Magnetic Materials, Vol.194, pp.83-89.

Le Renard, P.-E.; Jordan, O.; Faes, A.; Petri-Fink, A.; Hofmann, H.; Rüfenacht, D.; Bosman, F.; Buchegger, F. & Doelker, E. (2010). The *in vivo* performance of magnetic particle-loaded injectable, in situ gelling, carriers for the delivery of local hyperthermia, Biomaterials, Vol.31, pp.691–705.

Lee, E.-H.; Kim, C.-Y. & Choa, Y.-H. (2012). Magnetite nanoparticles dispersed within nanoporous aerogels for hyperthermia Application, Current Applied Physics, 2012, doi:10.1016/j.cap.2012.02.017, impress.

Lee, J.; Isobe, T. & Senna, M. (1996). Magnetic properties of ultrafine magnetite particles and their slurries prepared via in-situ precipitation, Colloids and Surfaces A: Physicochemical and Engineering Aspects, Vol.109, pp.121-127.

Lee, J.-H.; Schneider, B.; K. Jordan, E.; Liu, W. & Frank, J. A. (2008). Synthesis of complexable fluorescent superparamagnetic iron oxide nanoparticles (FL SPIONs) and its cell labeling for clinical application, Advanced Material, Vol.20, pp.2512-2516.

Lee, K.-J.; An, J.-H.; Shin, J.-S.; Kim, D.-H.; Yoo, H.-S. & Cho, C.-K. (2011). Biostability of γ-Fe2O3 nanoparticles Evaluated using an *in vitro* cytotoxicity assays on various tumor cell lines, Current Applied Physics, Vol.11, pp.467-471.

Li, L.; Chen, D.; Zhang, Y.; Deng, Z.; Ren, X.; Meng, X.; Tang, F.; Ren, J. & Zhang, L. (2007). Magnetic and fluorescent multifunctional chitosan nanoparticles as a smart drug delivery system, Nanotechnology, Vol.18, pp.405102-08.

Liao, C.; Sun, Q.; Liang, B.; Shen, J. & Shuai, X. (2011). Targeting EGFR-overexpressing tumor cells using cetuximab-immunomicelles loaded with doxorubicin and superparamagnetic iron oxide, European Journal of Radiology, Vol.80, pp.699-705.

Liu, R.-t.; Liu, J.; Tong, J.-q.; Tang, T.; Kong, W.-C.; Wang, X.-w.; Li, Y. & Tang, J.-t. (2012). Heating effect and biocompatibility of bacterial magnetosomes as potential materials used in magnetic fluid hyperthermia, Progress in NaturalScience: Materials International, Vol.22, pp.31-39.

Ma, J.; Chen, D.; Tian, Y. & Tao, K. (2000). Toxicity of Magnetic Albumin Microspheres Bearing Adriamycin, Journal of Tongji Medical University, Vol.202, pp.261-262.

Ma, M.; Zhang, Y.; Yu, W.; Shen, H.-y.; Zhang, H.-q. & Gu, N. (2003). Preparation and characterization of magnetite nanoparticles coated by amino silane, Colloids and Surfaces A: Physicochemical and Engineering Aspects, Vol.212, pp.219-226.

Madani, M.; Sharifi-Sanjani, N. & Faridi-Majidi, R. (2011). Magnetic polystyrene nanocapsules with core–shell morphology obtained by emulsifier-free miniemulsion polymerization, Polymer Science, Ser. A, Vol.53, pp.143-148.

Mahmoudi, M.; Sant, S.; Wang, B.; Laurent, S. & Sen, T. (2011). Superparamagnetic iron oxide nanoparticles (SPIONs): Development, surface modification and applications in chemotherapy, Advanced Drug Delivery Reviews, Vol.63, pp.24–46.

Mahmoudi, M.; Simchi, A.; Imani, M.; Milani, A.S. & Stroeve, P. (2009). An *in vitro* study of bare and poly(ethylene glycol)-co-fumarate coated superparamagnetic iron oxide nanoparticles: a new toxicity identification procedure, Nanotechnology, Vol.20, pp. 225104.

Mahmoudi, M.; Simchi, A.; Imani, M.; Shokrgozar, M.A.; Milani, A.S.; Häfeli, U.O. & Stroeve, P. (2010). A new approach for the *in vitro* identification of the cytotoxicity of superparamagnetic iron oxide nanoparticles, Colloids and Surfaces B: Biointerfaces, Vol.75, pp.300–309.

Mahmoudi, M.; Simchi, A.; Milani, A.S. & Stroeve, P. (2009). Cell toxicity of superparamagnetic iron oxide nanoparticles, Journal of Colloid and Interface Science, Vol.336, pp.510-518.

Maier-Hauff, K.; Ulrich, F.; Nestler, D.; Niehoff, H.; Wust, P.; Thiesen, B.; Orawa, H.; Budach, V. & Jordan, A. (2011). Efficacy and safety of intratumoral thermotherapy using magnetic iron-oxide nanoparticles combined with external beam radiotherapy on patients with recurrent glioblastoma multiforme, Journal of Neuro-Oncology, Vol.103, pp.317-324.

Mangual, J.O.; Aviles, M.O.; Ebner, A.D. & Ritter, J.A. (2011). *In vitro* study of magnetic nanoparticles as the implant for implant assisted magnetic drug targeting, Journal of Magnetism and Magnetic Materials, Vol.323, pp.1903-1908.

Martín-Saavedra, F.M.; Ruíz-Hernández, E.; Boré, A.; Arcos, D.; Vallet-Regí, M. & Vilaboa, N. (2010). Magnetic mesoporous silica spheres for hyperthermia therapy, Acta Biomaterialia, Vol.6, pp.4522-4531.

Meenach, S.A.; Hilt, J.Z. & Anderson, K.W. (2010). Poly(ethylene glycol)-based magnetic hydrogel nanocomposites for hyperthermia cancer therapy, Acta Biomaterialia, Vol.6, pp.1039-46.

Mishima, F.; Takeda, S.; Izumi, Y. & Nishijima, S. (2007). Development of Magnetic Field Control for Magnetically Targeted Drug Delivery System Using a Superconducting Magnet, IEEE Transactions on Applied Superconductivity, Vol.17, pp.2303-2306.

Miyazaki, T.; Miyaoka, A.; Ishida, E.; Li, Z.; Kawashita, M. & Hiraoka, M. (2012). Preparation of ferromagnetic microcapsules for hyperthermia using water/oil emulsion as a reaction field, Materials Science and Engineering C, Vol.32, pp.692-696.

Moroz, P.; Pardoe, H.; Jones, S.K.; St Pierre, T.G.; Song, S. & Gray, B.N. (2002). Arterial embolization hyperthermia: hepatic iron particle distribution and its potential determination by magnetic resonance imaging, Physics in Medicine and Biology, Vol.47, pp.1591-1602.

Muldoon, L.L.; Sandor, M.; Pinkston, K.E. & Neuwelt, E.A. (2005). Imaging, distribution, and toxicity of superparamagnetic iron oxide magnetic resonance nanoparticles in the rat brain and intracerebral tumor, Neurosurgery, Vol.57, pp.785-796.

Novakova, A.A.; Lanchinskaya, V.Yu.; Volkov, A.V.; Gendler, T.S.; Kiseleva, T.Yu.; Moskvina, M.A.& Zezin, S.B. (2003). Magnetic properties of polymer nanocomposites containing iron oxide nanoparticles, Journal of Magnetism and Magnetic Materials, Vol.258, pp.354-357.

Panczyk, T.; Warzocha, T.P. & Camp, P.J. (2010). A magnetically controlled molecular nanocontainer as a drug delivery system: The effects of carbon nanotube and magnetic nanoparticle parameters from monte carlo simulations, The Journal of Physical Chemistry C, Vol.114, pp.21299-21308.

Pardoe, H.; Clark, P.R.; St. Pierre, T.G.; Moroz, P. & Jones, S.K. (2003). A magnetic resonance imaging based method for measurement of tissue iron concentration in liver arterially embolized with ferromagnetic particles designed for magnetic hyperthermia treatment of tumors, Magnetic Resonance Imaging, Vol.21, pp.483-488.

Park, J.-H.; Im, K.-H.; Lee, S.-H.; Kim, D.-H.; Lee, D.-Y.; Lee, Y.-K.; Kim, K.-M. & Kim, K.-N. (2005). Preparation and characterization of magnetic chitosan particles for hyperthermia application, Journal of Magnetism and Magnetic Materials, Vol.293, pp.328–333.

Pisanic, T.R. 2nd; Blackwell, J.D.; Shubayev, V.I.; Finones, R.R. & Jin, S. (2007). Nanotoxicity of iron oxide nanoparticle internalization in growing neurons, Biomaterials, Vol.28, pp.2572–2581.

Pradhan, P.; Giri, J.; Rieken, F.; Koch, C.; Mykhaylyk, O.; Döblinger, M.; Banerjee, R.; Bahadur, D. & Plank, C. (2010). Targeted temperature sensitive magnetic liposomes for thermo-chemotherapy, Journal of Controlled Release, Vol.142, pp.108-121.

Purushotham, S.; Chang, P.E.J.; Rumpel, H.; Kee, I.H.C.; Ng, R.T.H.; Chow, P.K.H.; Tan, C.K. & Ramanujan, R.V. (2009). Thermoresponsive core–shell magnetic nanoparticles for combined modalities of cancer Therapy, Nanotechnology, Vol.20, pp.305101-12.

Purushotham, S. & Ramanujan, R.V. (2010). Thermoresponsive magnetic composite nanomaterials for multimodal cancer therapy, Acta Biomaterialia, Vol.6, pp.502-510.

Qui, X.-p. & Winnik, F. (2000). Preparation and characterization of PVA coated magnetic nanoparticles Chinese journal of polymer science, Vol.18, pp.535-539.

Raju, H.B.; Hu, Y.; Vedula, A.; Dubovy, S.R. & Goldberg, J.L. (2011). Evaluation of magnetic micro- and nanoparticle toxicity to ocular tissues, PLoS One, Vol.6, pp.e17452-63.

Raynal, I.; Prigent, P.; Peyramaure, S.; Najid, A.; Rebuzzi, C. & Corot, C. (2004). Macrophage endocytosis of superparamagnetic iron oxide nanoparticles: mechanisms and comparison of ferumoxides and ferumoxtran-10, Investigative Radiology, Vol.39, pp.56-63.

Rivera, G.P.; Huhn, D.; del Mercato, L.L.; Sasse, D. & Parak, W.J. (2010). Nanopharmacy: Inorganic nanoscale devices as vectors and active compounds, Pharmacological Research, Vol.62, pp.115-25.,

Ruiz-Hernandez, E.; Baeza, A. & Vallet-Regi, M. (2011). Smart Drug Delivery through DNA/Magnetic Nanoparticle Gates, American Chemical Society, Vol.5, pp.1259-1266.

Saavedra, F.M.; Ruíz-Hernández, E.; Boré, A.; Arcos, D.; Vallet-Regí, M. & Vilaboa, N. (2010). Magnetic mesoporous silica spheres for hyperthermia therapy, Acta Biomaterialia, Vol.6, pp.4522-4531.

Sahu, S.K.; Maiti, S.; Pramanik, A.; Ghosh, S.K. & Pramanik, P. (2012). Controlling the thickness of polymeric shell on magnetic nanoparticles loaded with doxorubicin for targeted delivery and MRI contrast agent, Carbohydrate Polymers, Vol.87, pp.2593-2604.

Salloum, M.; Ma, R. & Zhu, L. (2008). An in-vivo experimental study of temperature elevations in animal tissue during magnetic nanoparticle hyperthermia, International Journal of Hyperthermia, Vol.24, pp.589-601.

Salloum, M.; Ma, R. & Zhu, L. (2009). Enhancement in treatment planning for magnetic nanoparticle hyperthermia: optimization of the heat absorption pattern, International Journal of Hyperthermia, Vol.25, pp.309-321.

Schweiger, C.; Pietzonka, C.; Heverhagen, J. & Kissel, T. (2011). Novel magnetic iron oxide nanoparticles coated with poly(ethylene imine)-g-poly(ethylene glycol) for potential biomedical application: Synthesis, stability, cytotoxicity and MR imaging, International Journal of Pharmaceutics Vol.408, pp.130-137.

Sharifi, I.; Shokrollahi, H. & Amiri, S. (2012). Ferrite-based magnetic nanofluids used in hyperthermia applications, Journal of Magnetism and Magnetic Materials, Vol.324, pp.903–915.

Shen, S.; Ren, J.; Chen, J.; Lu, X.; Deng, C. & Jiang, X. (2011). Development of magnetic multiwalled carbon nanotubes combined with near-infrared radiation-assisted desorption for the determination of tissue distribution of doxorubicin liposome injects in rats, Journal of Chromatography A, Vol.1218, pp. 4619-4626.

Shkilnyy, A.; Munnier, E.; Herve, K.; Souce, M.; Benoit, R.; Cohen-Jonathan, S.; Limelette, P.; Saboungi, M.-L.; Dubois, P. & Chourpa, I. (2010). Synthesis and Evaluation of Novel Biocompatible Super-paramagnetic Iron Oxide Nanoparticles as Magnetic Anticancer Drug Carrier and Fluorescence Active Label, Journal of Physical Chemistry C, Vol.114, pp.5850-5858.

Shundo, C.; Zhang, H.; Nakanishi, T. & Osaka, T. (2012). Cytotoxicity evaluation of magnetite (Fe3O4) nanoparticles in mouse embryonic stem cells, Colloids and Surfaces B: Biointerfaces, Vol.97, pp.221-225.

Sieben, S.; Bergemann, C.; LuKbbe, A.; Brockmann, B. & Rescheleit, D. (2001). Comparison of different particles and methods for magnetic isolation of circulating tumor cells, Journal of Magnetism and Magnetic Materials, Vol.225, pp.175-179.

Simioni, A.R.; Primo, F.L.; Rodrigues, M.M.A.; Lacava, Z.G.M.; Morais, P.C. & Tedesco, A.C. (2007). Preparation, Characterization and *in vitro* Toxicity Test of Magnetic Nanoparticle-Based Drug Delivery System to Hyperthermia of Biological Tissues, IEEE Transactions on Magnetics, Vol.43, pp.2459-2461.

Singh, N.; Jenkins, G.J.S.; Nelson, B.C.; Marquis, B.J.; Maffeis, T.G.G.; Brown, A.P.; Williams,P.M.; Wright, C.J. & Doak, S.H. (2012). The role of iron redox state in the genotoxicity of ultrafine superparamagnetic iron oxide nanoparticles, Biomaterials, Vol.33, pp.163-170.

Skumiel, A. (2006). Suitability of water based magnetic fluid with CoFe2O4 particles in hyperthermia, Journal of Magnetism and Magnetic Materials, Vol.307, pp.85-90.

Su, W.; Wang, H.; Wang, S.; Liao, Z.; Kang, S.; Peng, Y.; Han, L. & Chang, J. (2012). PEG/RGD-modified magnetic polymeric liposomes for controlled drug release and tumor cell targeting, International Journal of Pharmaceutics, Vol.426, pp.170-181.

Sun, Y.; Chen, Z.; Yang, X.; Huang, P.; Zhou, X. & Du X. (2009). Magnetic chitosan nanoparticles as a drug delivery system for targeting photodynamic therapy, Nanotechnology, Vol.20, pp.135102-10.

Thunemann, A.F.; Schutt, D.; Kaufner, L.; Pison, U. & Mohwald, H. (2006). Maghemite Nanoparticles Protectively Coated with Poly(ethylene imine) and Poly(ethylene oxide)-block-poly(glutamic acid), Langmuir, Vol.22, pp.2351-2357.

Tung, W.L.; Hu, S.H. & Liu, D.M. (2011). Synthesis of nanocarriers with remote magnetic drug release control and enhanced drug delivery for intracellular targeting of cancer cells, Acta Biomaterialia, Vol.7, pp.2873-2882.

Urbina, M.C.; Zinoveva, S.; Miller, T.; Sabliov, C.M.; Monroe, W.T. & Kumar, C.S.S.R. (2008). Investigation of Magnetic Nanoparticle-Polymer Composites for Multiple-controlled Drug Delivery, The Journal of Physical Chemistry C, Vol.112, pp.11102–11108.

Van der Zee, J. (2002). Heating the patient: a promising approach?, Annals of Oncology, Vol.13, pp.1173–1184.

Veiseh, O.; Gunn, J.W. & Zhang M. (2010). Design and fabrication of magnetic nanoparticles for targeted drug delivery and imaging, Advanced Drug Delivery Reviews, Vol.62, pp.284–304.

Vermisoglou, E.C.; Pilatos, G.; Romanos, G.E.; Devlin, E.; Kanellopoulos, N.K. & Karanikolos, G.N. (2011). Magnetic carbon nanotubes with particle-free surfaces and high drug loading capacity, Nanotechnology, vol.22, pp.355602-12.

Voit, W.; Kim, D.K.; Zapka, W.; Muhammed, M. & Rao, K.V. (2001). Magnetic behavior of coated superparamagnetic iron oxide nanoparticles in ferrofluids, Materials Research Society Symposium Proceedings, Vol. 676, pp.Y7.8.1- Y7.8.6.

Wang, H.; Wang, S.; Liao, Z.; Zhao, P.; Su, W.; Niu, R. & Chang, J. (2012). Folate-targeting magnetic core–shell nanocarriers for selective drug release and imaging, International Journal of Pharmaceutics, Vol.430, pp.342-349.

Wang, L.; Neoh, K.G.; Kang, E.-T. & Shuter, B. (2011). Multifunctional polyglycerol-grafted Fe3O4@SiO2 nanoparticles for targeting ovarian cancer cells, Biomaterials, Vol.32, pp.2166-2173.

Winer, J.L.; Liu, C.Y. & Apuzzo, M.L.J. (2011). The Use of Nanoparticles as Contrast Media in Neuroimaging: A Statement on Toxicity, World Neurosurgery, DOI:10.1016/j.wneu.2011.08.013, impress.

Wu, H.; Liu, G.; Wang, X.; Zhang, J.; Chen, Y.; Shi, J.; Yang, H.; Hua, H. & Yang, S. (2011). Solvothermal synthesis of cobalt ferrite nanoparticles loaded on multiwalled carbon nanotubes for magnetic resonance imaging and drug delivery, Acta Biomaterialia, Vol.7, pp.3496-3504.

Wust, P.; Hildebrandt, B.; Sreenivasa, G.; Rau, B.; Gellermann, J.; Riess, H.; Felix, R. & Schlag, P.M. (2002). Hyperthermia in combined treatment of cancer, The Lancet Oncology, Vol.3, pp.487–497.

Wust, P.; Hildebrandt, B.; Sreenivasa, G.; Rau, B.; Gellermann, J.; Riess, H.; Felix, R. & Schlag, P.M. (2002). Hyperthermia in combined treatment of cancer. The Lancet Oncology Vol.3, pp.487–497.

Yallapu, M.M.; Othman, S.F.; Curtis, E.T.; Gupta, B.K.; Jaggi, M. & Chauhan, S.C. (2011). Multi-functional magnetic nanoparticles for magnetic resonance imaging and cancer therapy, Biomaterials, Vol.32, pp.1890-1905.

Yang, F.; Fu, D.L.; Long, J. & Ni, Q.X. (2008). Magnetic lymphatic targeting drug delivery system using carbon nanotubes, Medical Hypotheses, Vol.70, pp.765-767.

Yang, F.; Jin, C.; Yang, D.; Jiang, Y.; Li, J.; Di, Y.; Hu, J.; Wang, C.; Ni, Q. & Fu, D. (2011). Magnetic functionalised carbon nanotubes as drug vehicles for cancer lymph node metastasis treatment, European Journal of Cancer, Vol.47, pp.1873-1882.

Yang, J.; Lee, H.; Hyung, W.; Park, S.-B. & Haam, S. (2006). Magnetic PECA nanoparticles as drug carriers for targeted delivery: Synthesis and release characteristics, Journal of Microencapsulation, Vol.23, pp.203-212.

Yang, Q.; Liang, J. & Han, H. (2009). Probing the Interaction of Magnetic Iron Oxide Nanoparticles with Bovine Serum Albumin by Spectroscopic Techniques, The Journal of Physical Chemistry B, Vol. 113, pp.10454-10458.

Yang, X.; Hong, H.; Grailer, J.J.; Rowland, I.J.; Javadi, A.; Hurley, S.A.; Xiao, Y.; Yang, Y.; Zhang, Y.; Nickles, R.J.; Cai, W.; Steeber, D.A. & Gong, S. (2011). cRGD-functionalized, DOX-conjugated, and ^{64}Cu-labeled superparamagnetic iron oxide nanoparticles for targeted anticancer drug delivery and PET/MR imaging, Biomaterials, Vol.32, pp.4151-4160.

Yang, Y.; Jiang, J.S.; Du, B.; Gan, Z.F.; Qian, M. & Zhang, P. (2009). Preparation and properties of a novel drug delivery system with both magnetic and biomolecular targeting, Journal of Materials Science: Materials in Medicine, Vol.20, pp.301-307.

Yao, A.; Ai, F.; Wang, D.; Huang, W. & Zhang, X. (2009). Synthesis, characterization and in vitro cytotoxicity of self-regulating magnetic implant material for hyperthermia application, Materials Science and Engineering C, Vol.29, pp.2525-2529.

Yellen, B.B.; Forbes, Z.G.; Halverson, D.S.; Fridman, G.; Barbee, K.A.; Chorny, M.; Levy, R. & Friedman, G. (2005). Targeted drug delivery to magnetic implants for therapeutic applications, Journal of Magnetism and Magnetic Materials, Vol.293, pp.647-654.

Yildirimer, L.; Thanh, N.T.K.; Loizidou, M. & Seifalian, A.M. (2011). Toxicological considerations of clinically applicable Nanoparticles, Nano Today, Vol.6, pp.585-607.

Zefeng, X.; Guobin, W.; Kaixiong, T.; Jianxing, L. & Yuan, T. (2005). Preparation and acute toxicology of nano-magnetic ferrofluid, Journal of Huazhong University of Science and Technology -- Medical Sciences, Vol.25, pp.59-61.

Zhang, L.; Zhang, F.; Wang, Y.-S.; Sun, Y.-L.; Dong, W.-F.; Song, J.-F.; Huo, Q.-S. & Sun, H.-B. (2011). Magnetic colloidosomes fabricated by Fe_3O_4–SiO_2 hetero-nanorods, Soft Matter, Vol.7, pp. 7375-7381.

Zhang, Y.Q.; Li, L.L.; Tang, F. & Ren, J. (2006). Controlled Drug Delivery System Based on Magnetic Hollow Spheres/Polyelectrolyte Multilayer Core–Shell Structure, Journal of Nanoscience and Nanotechnology, Vol.6, pp.3210–3214.

Zhou, H.; Tao, K.; Ding, J.; Zhang, Z.; Sun, K. & Shi, W. (2011). A general approach for providing nanoparticles water-dispersibility by grinding with poly (ethylene glycol). Colloids and Surfaces A: Physicochemical and Engineering Aspects 2011; Vol.389, pp.18-26.